Chapter 3
Result
And
Discussion

Section A Batch study

3. Results and discussion

The present work includes Bio-remediation of benzene in free cell and packed bed reactors under optimized condition in batch (PBBR) and continuous (CPBBR) mode using bacterial species isolated from petroleum contaminated site. The characterizations of bacterial species were done using Biochemical and DNA techniques. The process parameters were optimized to get the better biodegradation rate. The performance of bioreactors was evaluated under varying process condition. The kinetic study, identification of metabolites and predication of bio-degradation pathway, and analysis of identified Proteins by bioinformatics servers and tools were also carried out. The results are presented in subsequent sections and sub-sections of this chapter.

3.1 Isolation and characterization (morphological, biochemical and molecular16s-rRNA)

The nature of the bacterial isolates was found to be of mobile and rod-shape with the help of lab microscope (Dewinter Tech, India). The SEM images assured that the isolates were nearly regular and rod-shape. The results of biochemical characterization of micro-organism through standard procedure as per Bergy's resulted +ve for Ureas, Voges-Proskauer, Oxidase, Catalase, Gram's staining and negative for Indole production, Methyl Red and fermentation. The characteristics of bio-chemical tests were given in **Table .5**.

Molecular investigation of the microbial isolates provides better observation and quantification of genealogical variety because it is very discrete and responsive in

comparison to any biological method. The molecular investigation of the bacterial isolates was carried out with products of amplified PCR of 1.5Kb size which guaranteed 16SrRNA presence. The 16SrRNA gene sequences were arranged according to NCBI database which showed almost 99.0% of resemblance with Bacillus species M_4 (Fig.16). The outcomes indicated that the subfamily of Bacillus species were main element and thus associated in benzene biotransformation. The outcome was compatible with those of microscopic and SEM investigation that showed rod-shape and mobile nature of bacterial isolates. Previous studies showed that the bacterial isolates from oil sludge were from *Bacillus* species family (Liu et al., 2010; Kureel et al., 2016).

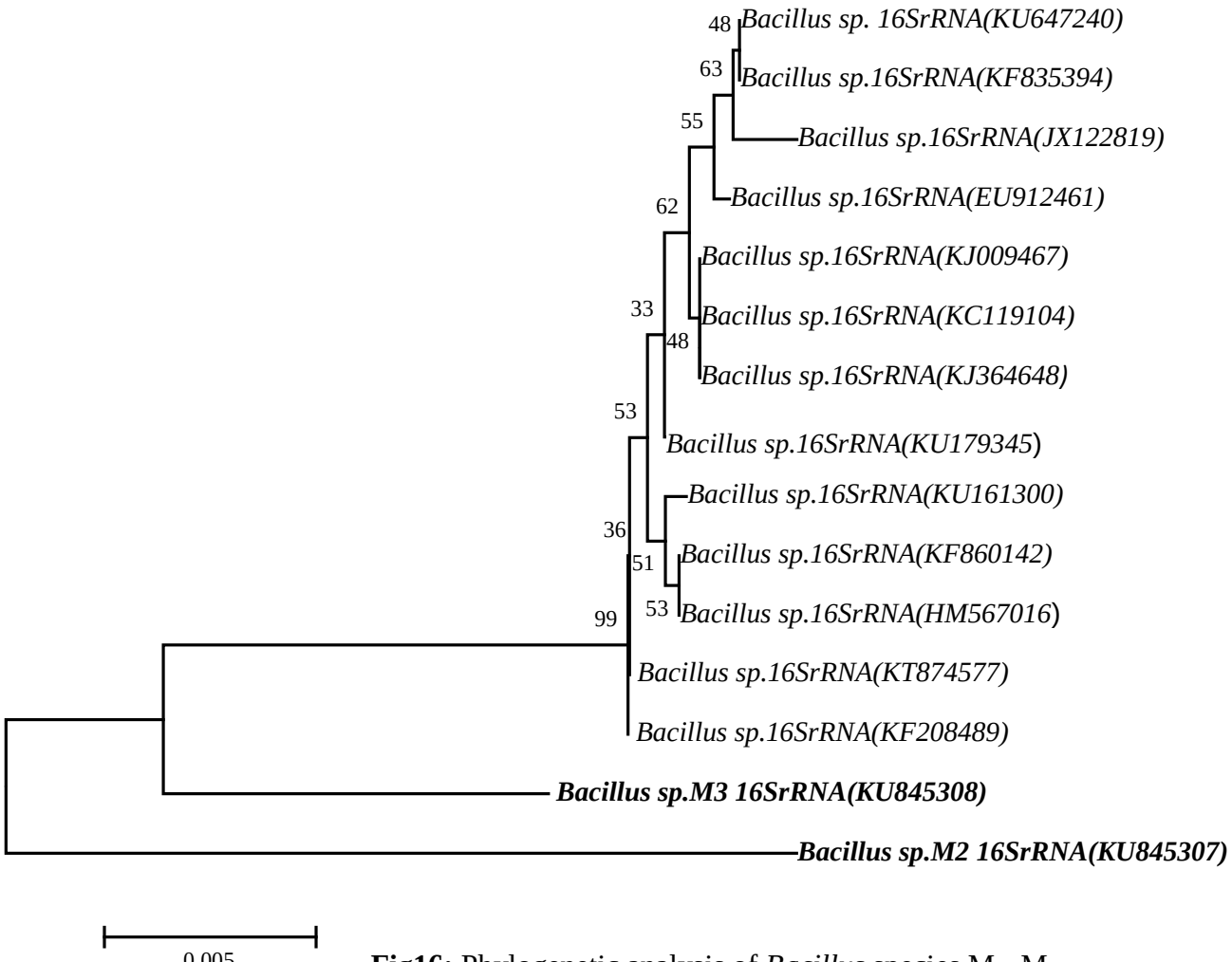

Fig16: Phylogenetic analysis of *Bacillus* species M_2, M_3

Table. 5 Biochemical testing for isolated species.

Analytical test	Bacillus sp. M2	Bacillus sp. M3	Bacillus sp. M4
Cell	rod shaped,	rod shaped,	rod shaped,
Gram staining	Gram- positive	Gram- positive	Gram- positive
Motility	+	+	+
Catalase	+	+	+
Voges-Proskauer	-	+	+
Methyl red	+	-	-
Indole	-	-	-
Urease	+	+	+
Fermentation test			
Glucose			
Maltose	+	+	+
Sucrose	+	+	+
Lactose	+	+	+
Mannitol	+	+	+
	+	+	+

3.2 Optimization of process parameters and screening of potential microbial species for biodegradation of benzene

Temperature, pH and inoculums size (quantity of species) were optimized. The optimal values were found to be 37.0 ^{0}C, 7.0 and 6.0 × 10^8 CFU/mL respectively and used in the subsequent experimental work. Under optimal conditions 92% and 81% of benzene removal was observed in a ten days of free-cell batch experiment by *Bacillus* species M_2 and M_3 at an initial concentration of 250 and 200 mg/L respectively. Above this concentration, the bio-degradation rate started decreasing that indicated the presence of

possible inhibition in process. The results clearly indicated that Bacillus species M_3 has higher benzene degrading potential as compared to Bacillus species M_2. Therefore, bacillus species M_3 was preferred over Bacillus species M_2 for further degradation study in the packed bed bio-reactor.

3.3 Comparing the performance of free cell vs. immobilized packed (alginate and PUF) bed bioreactor for degradation of Benzene

Fig: 17 (a-d) unveils benzene degradation in immobilized PBBR (PUF as well as alginate beads) and free cell at various initial concentration. The fluctuation in dry cell weight indicates growth of bacteria by utilization of benzene as main carbon source. The dry cell weight correlating with each concentration was measured with time and plotted on secondary y-axis as shown in Fig 17 (a-c). Fig (17d) indicates comparison of benzene degradation within free cell, PUF and alginate beads at same initial concentration of 400 mg/L.

A benzene degradation graph of free cell v/s % removal of benzene per day is shown in Fig (17a) with varying concentration range of 100-500 mg/L. A maximum of 92 % removal was noticed with initial benzene concentration of 250 mg/L. When benzene's initial concentration rose to 400 mg/L, the maximum removal of 70% was achieved on the eighth day of operation. When the starting concentration was 500 mg/L, the free-cell batch system practically failed in degrading benzene (30% removal). Shim and Yang. (1999) also reported failure in degrading benzene at ~500 mg/L in free-cell. This might be because of direct contact of very high benzene concentration to bacterial species in free-cell while in an immobilized-system the bacteria is more evenly distributed due to availability of very high surface area and benzene has to pass through different film resistances (liquid and

biofilm) in order to reach the bacterial cell and therefore concentration reduces remarkably when benzene came in contact with bacteria (Shim and Yang, 1999; Singh and Fulekar, 2010). Singh and Fulekar (2010). The packed bed reactor reported 67.5% of removal benzene at initial concentration of 500 mg/L in 168 h by P. *putida*. Substrate inhibition was started above 500 mg/L. Hamed et al., (2003) noticed 65% benzene removal at an initial concentration of 420 mg/L by P. *putida* while Robledo-Ortíz et al., (2011) found 60 to 99 % of BTX removal with starting concentration ranging from 15 to 90 mg/L by P. *putida* F1 in free-cells.

Alginate beads were directly used as a packing media in the PBBR after preparation. However, polyurethane foam pieces were rinsed by solution having 6.0×10^{8} CFU/mL of *Bacillus* species M_3 along with necessary carbon and nutrients source so that bacterial population gets immobilized on PUF surface**.** Less degradation was noticed in the initial phase (<1 day) but after that the degradation rate increased and became practically steady upto 8^{th} day and then started declining. Fig: 17b and 17c shown 84% and 90% of benzene biodegradation after 9 days with an initial benzene concentration of 400 mg/L in PBBR packed with alginate beads and immobilized PUF respectively. This study also revealed that PBBR (immobilized systems) has greater potential to remove benzene in comparison to free-cell system (70% at 400 mg/L) as the reaction rate was speed up by the native cell population on the immobilized mold **(**Singh et al., 2010; Padmanaban et al., 2016**).** With benzene concentration of 500 mg/L, the free-cell batch system practically failed in degrading benzene (30% RE) while immobilized systems (alginate beads and PUF) were still active in removing benzene upto 1200 mg/L (33% RE) and 900 mg/L (37% RE) respectively. These results justify that for large scale operations the packed bed systems with immobilized bacterial species are more suitable (Fig. 17a-c).

The reason for better biodegradation of benzene in PUF packed PBBR over alginate beads might be due to large surface area or active sites and better holding strength of immobilized-cells on polyurethane foam. These reasons might have provided better bacterial activity on PUF immobilized-cells (Patil et al., 2003; Patil et al., 2006). The poor strength and stability of alginate-immobilized cells may be another reason, which resulted in leakage of cell from alginate beads (Patil et al., 2006).

The best indicator of favorable condition supplied by packed material for the multiplication and growth of micro-organism is change in CFU. The measurement of CFU in the PBBR packed with alginate beads and PUF were done when maximum degradation was achieved and which came out to be 8.0×10^{6}CFU/mL and 6.0×10^{6}CFU/mL respectively. The increment in CFU/mL count in regular interval for both the systems indicated that both packing provided favorable environment for bacterial-cell growth (Yadav et al., 2014; Kureel et al., 2016; Geed et al., 2017; Padmanaban et al., 2016).

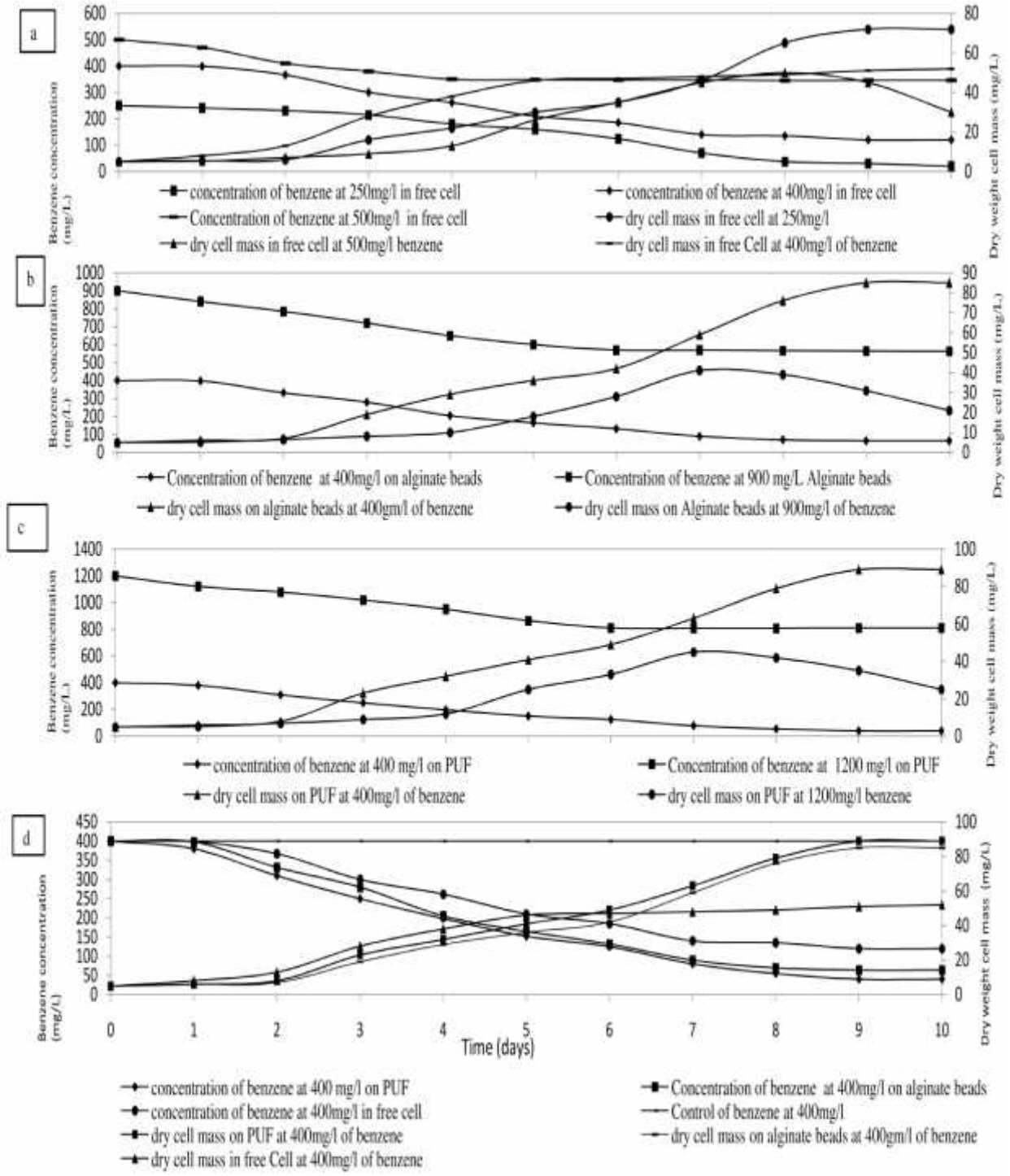

Fig.17: Representation of biodegradation of benzene in free (a), immobilized cells on Alginate beads and PUF (b) and (c), Fig (d) shows comparison in between free, immobilized on Alginate beads and PUF at concentration of benzene 400 mg/L.

3.4. SEM, FT-IR and GC/MS analysis

The images of SEM of polyurethane foam and sodium alginate bead without immobilization and ten days after immobilization and benzene as sole carbon source are shown in Fig. 18(a-d). Some evident of formation of biofilm and presence of bacteria on the surface of the packing material are visible however more experiments are required to confirm this fact.

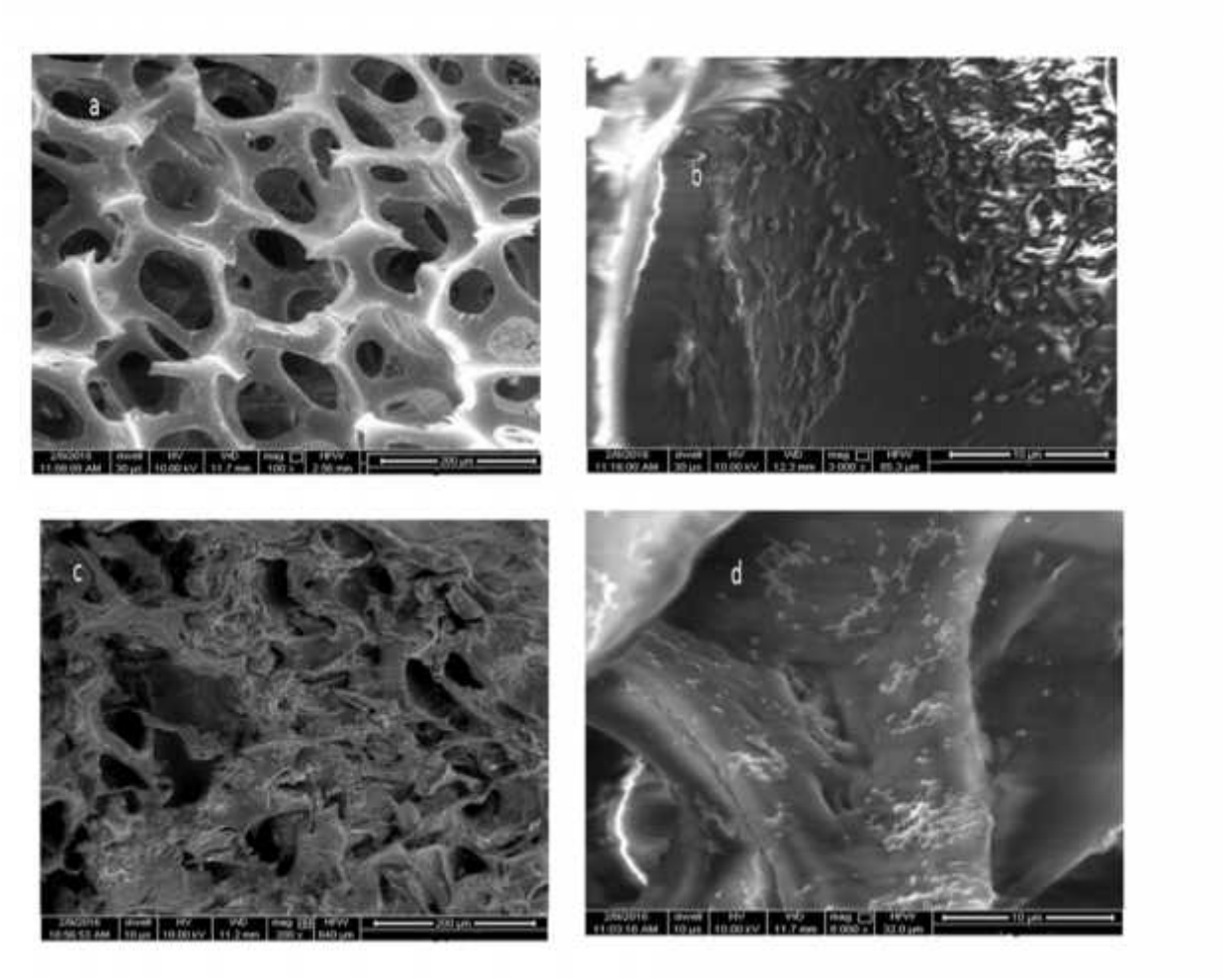

Fig18: SEM images of polyurethane foam and sodium alginate bead (a, c) polyurethane-foam-immobilized cells (PFIC) (b) Sodium alginate bead immobilized cell (d)

From the FT-IR outcomes, peaks corresponding to range of 3345.1 to 3400.3(1/cm) and 1643.3 1/cm were obtained which assured presence of hydroxyl (-OH) and carbonyl groups (=C=O). This clearly indicates that benzene was successfully bio-oxidized in the liquid phase. Along with above groups, some peaks were in range of 662.4 to 3994.1 (1/cm) which corresponds to 1, 2-benzenediol, hydroquinone, benzoate and phenol functional groups. The stable metabolites formed as a result of the degradation of benzene may be associated with these additional groups (Fig 19 a,b). However for the confirmation of results, further investigations were done by GC-MS analysis. Benzene's band spectrum was 1815.0 (1/cm) for the control sample. The outcomes were in accordance with those described by Robledo-Ortiz et al. (2011) who also noticed similar functional groups by the use of FTIR. This might be characteristics of *Bacillus* species M_3, which obeys a particular catabolic pathway for degradation of benzene (Reardon et al., 2000; Yu et al., 2001).

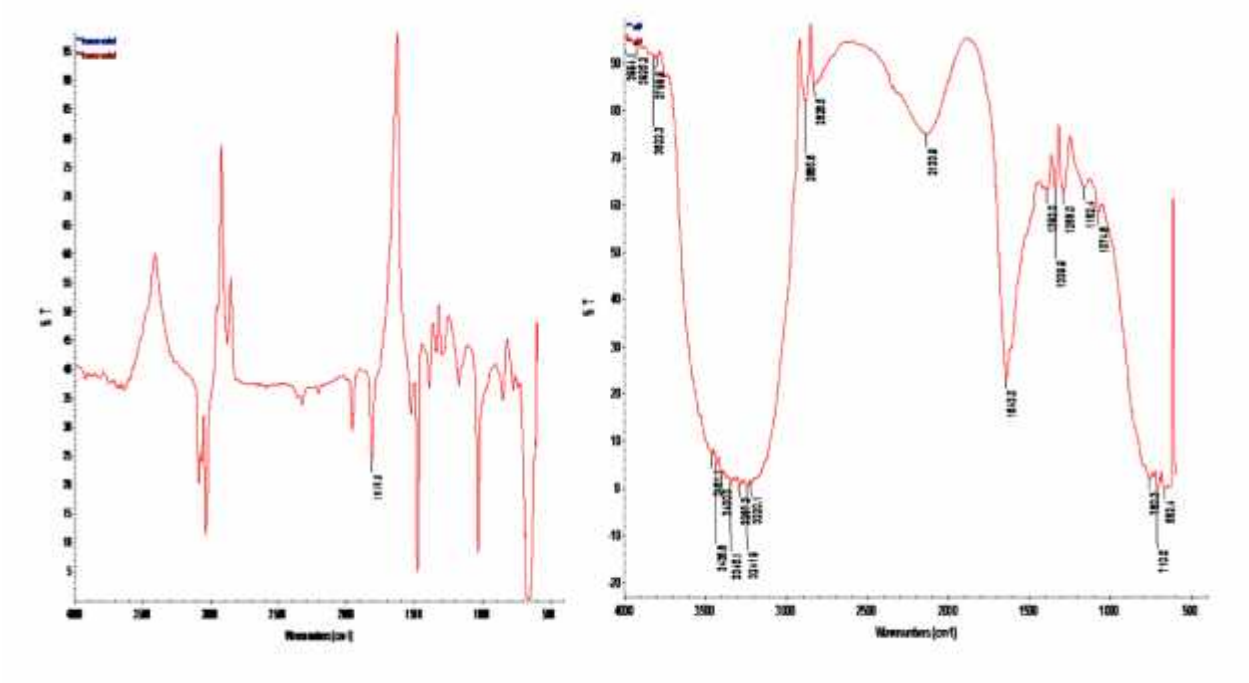

Fig19: Band position of (a) control sample (benzene) (b)biodegraded sample

The samples extracted by n-hexane were analyzed (Fig. 20 a-e) using GC-MS technique. The outcome confirmed the existence of benzene along with 4 other compounds (perhaps metabolites) within the samples during ten days of inoculation. The data of mass-spectra procured by GC-MS were emulated with that of NIST library and mass upon charge ratio (m/z) of 94, 66 and 39 were obtained. The result was identical with phenolic compounds as shown in (Fig. 20b). Another three metabolites which were recognized by fragmentation pattern are following at m/z 122, 105, 77, 51 (benzoate); 110, 92, 81, 64 (1, 2-benzenediol); and m/z 110, 81, 55, 39(hydroquinone). The outcomes of GC-MS chromatographic and fragmented results were depicted in Fig 20(a-e) and Fig 21.

The outcomes affirmed the detections of FTIR and indicated that there is feasibility of 1,2-benzenedi-ol,phenol, benzoate and hydroquinone as intermediary from aerobic oxidation of benzene by strain *Bacillus* species M_3. The outcome is emulating with various suitable pathways suggested by numerous researchers for benzene's metabolism including hydroxylation and carboxylation to yield benzoate, 1,2-benzenediol,, phenol and hydroquinone respectively in presence of oxygen (Caldwell and Joseph, 2000; Dou et al., 2010;Robledo-Ortíz et al., 2011).

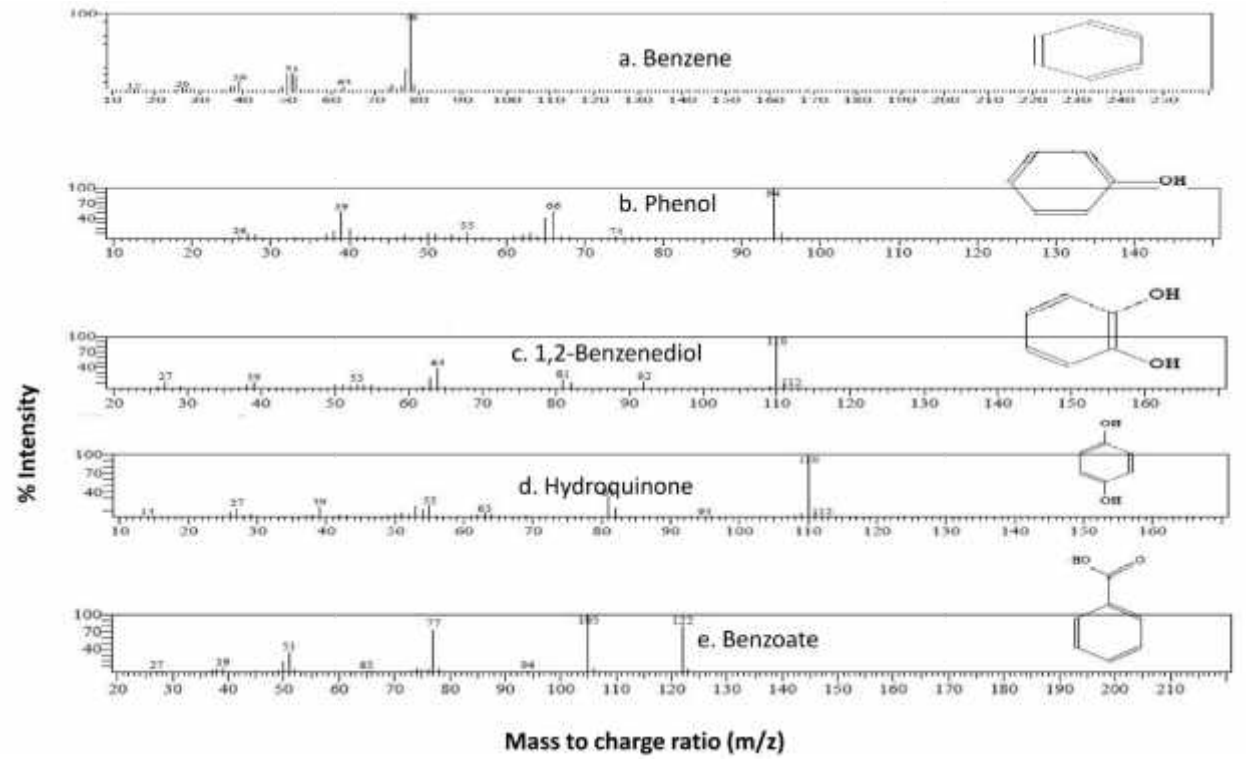

Fig 20: Mass spectrum of a) benzene (m/z identification 78); (b) phenol (m/z identification 94, 66, 39); (c) 1,2-benzenediol (m/z identification 110, 92, 81, 64); (d) hydroquinone (m/z identification 110, 81, 55, 39) and (e) Benzoate (m/z identification 122, 105, 77, 51).

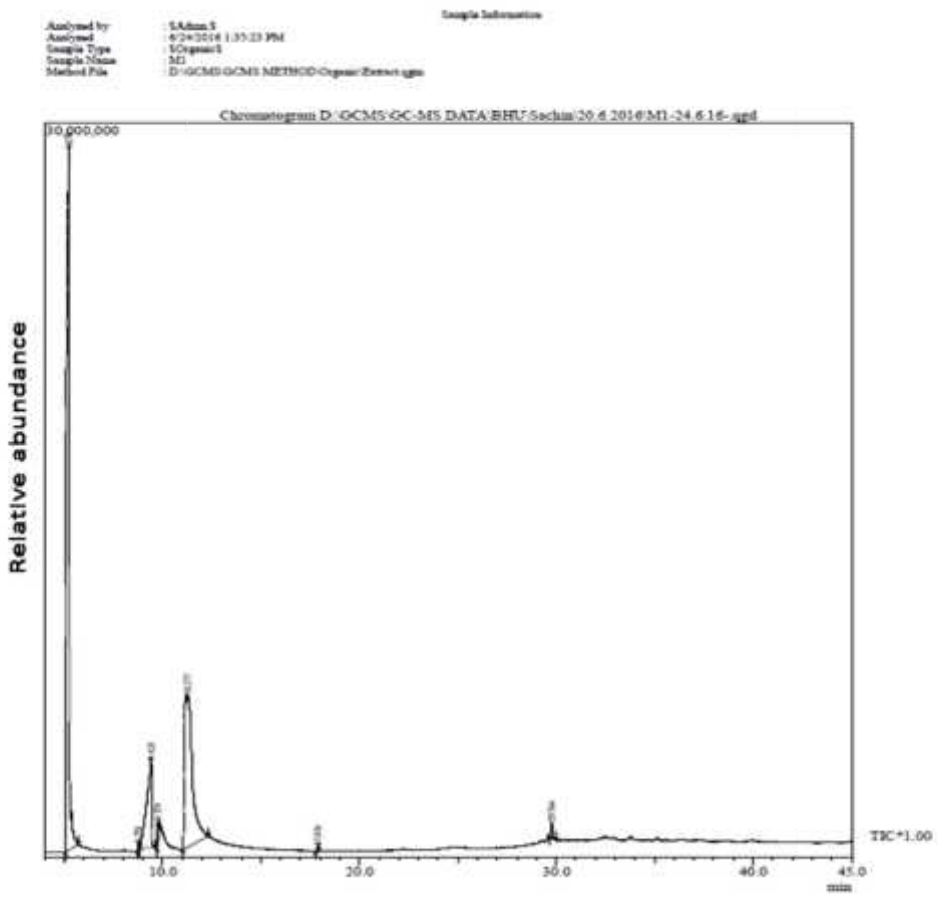

Fig. 21: GC-MS Chromatogram analysis of biodegraded sample of benzene

3.5. Growth and inhibition kinetics for biodegradation of benzene

In order to calculate kinetic parameters of immobilized and free cells bioreactors with Bacillus species M_3, Monod growth kinetic model was used at concentration of 250 mg/L and 400 mg/L respectively. μ_{max} and K_s values were calculated and found to be 0.247 1/day, 154.94 mg/L; 0.296 1/day, 143.81mg/L and 0.179 1/day, 144.86 mg/L for Alginate beads, Polyurethane foam and free cell respectively (Fig. 22a**; Table. 6**). Since μ_{max}/K_s is a more reasonable parameter which show the effectiveness of bioreactor system with low value of K_s and high value of μ_{max} as desirable condition for biodegradation (Kovarova-Kovar and Egli, 1998; yadav et al., 2014; Geed et al., 2017). In the current

work, μ_{max}/ K_s value for cells immobilized on PUF and alginate as well as free cell were calculated and found to be 0.00159, 0.00206 and 0.00123, respectively. On the basis of these ratios, it can be concluded that the immobilized systems are more efficient in remediation of benzene in comparison to free-cell system. Out of the two immobilized systems which were part of the current work, the performance of Polyurethane Foam based PBBR was better than alginate based PBBR under similar operating conditions. This certainly indicates the significance of packing media in bioremediation.

Liu et al. (2010) reported similar results in which they performed the kinetics of benzene degradation in free-cell system by *Bacillus* species at low concentration of 160 mg/L and found the values of K_s and μ_{max} as 4.26 mg/L and 2.225 L/hr, respectively. Robledo *et al* (2011) reported the values of μ_{max} and K_s for *Pseudomonas* putida (K_s= 10.11mg/L; μ_{max} = 0.50 L/hr) at concentration range of 30 to 90 mg/L in an immobilized polymer /agave-fiber/ foamed batch bioreactor system. The experimental research carried out by Liu et al. (2010) and Robledo *et al.* (2011) were at low benzene concentration in free cell and immobilized system. In the current work (low value K_s and high value of μ_{max}) the results obtained are better than that reported by Geed *et al.* (2017) (K_s; 126.3 mg/L and μ_{max}; 0.271 1/day) at high concentration of various pollutant by *Bacillus* species.

The outcome of free-cell system shows that benzene degradation rate declines at concentration above 250 mg/L for *Bacillus* species M_3 which clearly indicates the probability of inhibition and therefore Inhibition model should be applied to have precise kinetic parameters values beyond this concentration concentration. At high benzene concentration (substrate inhibition), kinetic parameters i.e. $\mu_{max,}$ K_s, and K_i were computed with the help of Haldane-Andrews inhibition model for alginate bead, polyurethane foam and free cell which came out to be 0.287 1/day, 240.87 mg/L and 664.25 mg/L; 0.296

1/day, 220.71 mg/L and 724.93 mg/L; 237 1/day, 143.40 mg/L and 435.84 mg/L; respectively (Fig.22b**, Table 6b**). In immobilized systems the values of inhibition constant were significantly greater than free-cell system as shown in Table 6 **(a, b)**. This result clearly indicates that the inhibitory condition delayed in packed bed immobilized system as compared to free cell system. This also indicates superiority of packed bed systems as compared to free cell systems. It was noticed that the value of μ_{max}/K_s (inhibition kinetics) for *Bacillus* species M_3 was 0.00119 in alginate, which was moderately lower than PUF (0.00134) in immobilized system.

Kim *et al.* (2005) calculated kinetic parameters with the help of inhibition kinetic model. With the help of inhibition model they computed kinetic parameters for *Pseudomonas* putida species (μ_{max}= 0.3 1/hr, K_i =100 mg/L, K_s = 30 mg/L) at concentration of 200 mg/L in free-cell system. Tsai *et al.* (2013) reported (μ_{max}= 0.1155 1/hr, K_i = 52.63 mg/L ,K_s = 4.93 mg/L) in free-cell and (μ_{max}= 0.4259 1/hr, K_i =5.46 mg/L ,K_s = 10.55 mg/L) in an immobilized glass-bottle system with concentration range 17.6 to 78.9 mg/L. Geed et al. (2017) found (μ_{max}= 0.315 1/day, K_i =594.75 mg/L,K_s = 151.32 mg/L) for various pollutants by Bacillus species. The notable difference in kinetic parameters computed by numerous researchers for identical species might be because of several reasons like cell history, cell growth condition, inoculums techniques, various operating conditions etc. The kinetic analysis is a mirror image of any organism's intrinsic characteristic and therefore these are difficult to reproduce under the existing environmental conditions.

Table 6 (a, b): Growth and inhibition kinetics parameter of Monod and Andrew-Halden model for biodegradation of benzene by *Bacillus* sp. M3

Monod growth kinetic parameters

Batch Systems	**Substrate Concentration range (mg/L)**	**μ_{max}(Per day)**	**K_s(mg/L)**	**μ_{max}/ K_s (L/ mg.day)**	**R^2**
Free cell	100-250	0.179	144.86	0.00123	0.9657
Immobilized alginate beads	100-400	0.247	154.94	0.00159	0.9489
Immobilized PUF	100-400	0.296	143.81	0.00206	0.9606

Andrew-Haldan inhibition kinetic parameters

Batch Systems	**Substrate Concentration range (mg/L)**	**μ_{max}(Per day)**	**Ks(mg/L)**	**μ_{max}/ K_s (L/ mg.day)**	**K_i (mg/L)**	**R^2**
Free cell	100-1500	0.237	143.4	0.00039	435.84	0.964
Immobilized alginate beads	100-1500	0.287	240.87	0.00119	664.25	0.954
Immobilized PUF	100-1500	0.296	220.71	0.00134	724.93	0.9803

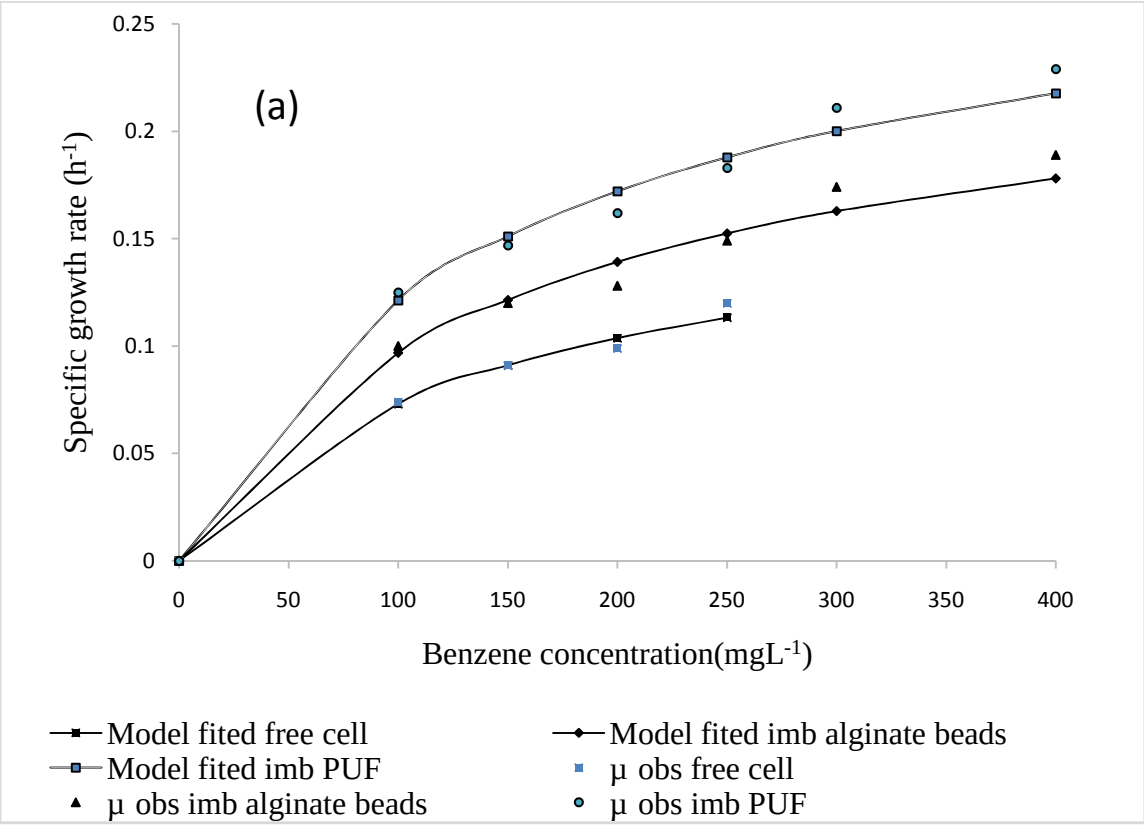
(a)
Specific growth rate (h-1)
0.25
0.2
0.15
0.1
0.05
0
0
50
100
150
200
250
300
350
400
Benzene concentration(mgL-1)
Model fited free cell
Model fited imb alginate beads
Model fited imb PUF
µ obs free cell
µ obs imb alginate beads
µ obs imb PUF

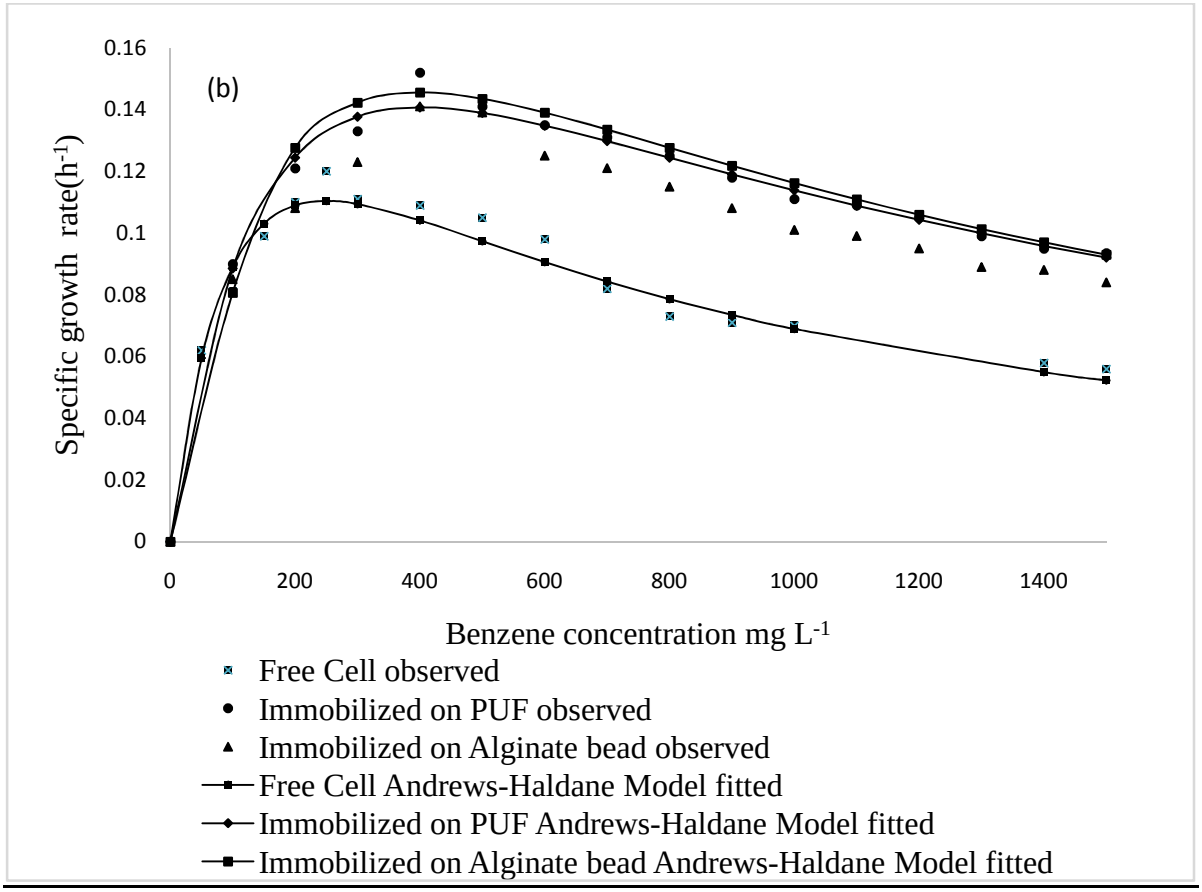

Fig 22:(a) Observed data of specific growth rate versus benzene substrate concentration and model fit using Monod Model. **(b)** Observed data of specific growth rate versus benzene substrate concentration and model fit using Andrew-Haldane.

Section B Continuous Study

3.6 Biochemical and molecular characterization (16S rRNA) of bacterial isolate

Bio-chemical analysis of micro-organism were done and results came out +ve for Oxidase, Urease, Fermentation, Voges-Proskauer, Gram's staining, Catalase and –ve for Indole production, Methyl red.

The molecular investigation of bacterial isolates provides better observation and quantification of genealogical variety because it is very discrete and responsive as compared to any biological approach. The molecular investigation of bacterial isolate was done with products of amplified PCR of 1.5 Kb sizes which guaranteed 16S rRNA gene presence. The 16S rRNA bacterial sequences were aligned according to NCBI databases which showed 95% of resemblance with *Bacillus* species M_4 (Fig. 23**)**. The preparation of phylogenetic tree is done with software named MEGA 6. The outcomes indicated that the Bacillus species genera were main element and thus associated in benzene biotransformation. These findings were validated by Liu et al (2010).

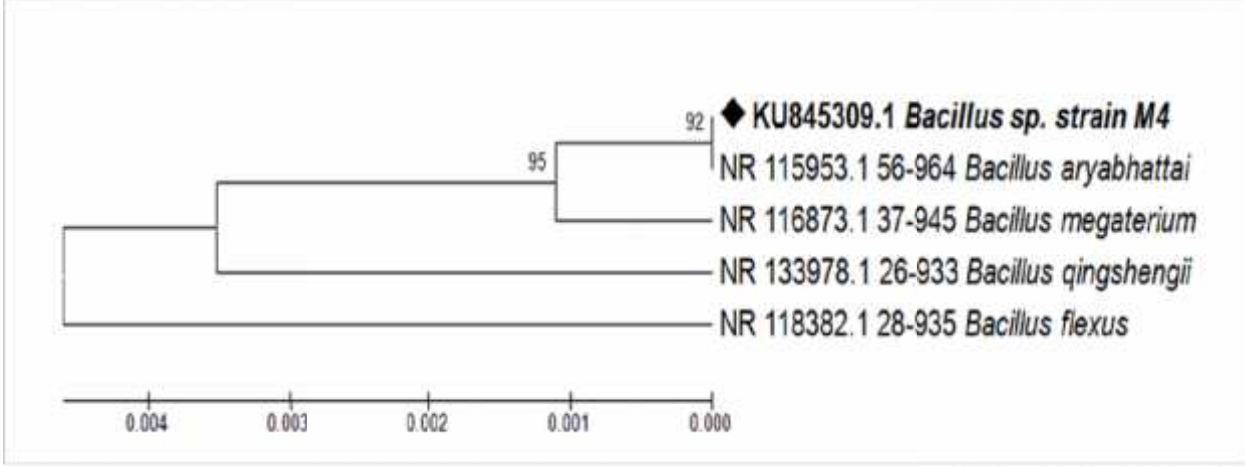

Fig23: Polygenetic tree of bacterial *Bacillus*sp.M4

3.7 Batch bioreactor immobilization study

The various process parameters were optimized experimentally and the performance of the reactor was evaluated under optimum condition at different concentrations and flow rate (CPBBR). In order to optimize pH, it was varied from 6.0 to 9.0 and its effect on removal of benzene was examined. The optimal value of pH was found to be 7.0 at which maximum percent removal of 95 % was achieved and shown in Fig 24a. DO was also optimized with the same procedure as above with varying DO level from 3.0 to 7.0 mg/L. It was noticed that percent removal efficiency increased upto 92.3% at 5.2 mg/L and afterwards it declined as presented in Fig 24b. Similarly Inoculums size was optimized by changing its size from 2.0×10^8 to 10.0×10^8 CFU/mL. A maximum removal of 93.1% was obtained at inoculum size of $8.0 * 10^8$ CFU/mL under room temperature was obtained as depicted in Fig 24c. The outcomes acquired in the current work were some where identical with the outcomes of Das *et al* (2014). The optimal value of DO, Inoculum size and pH came out to be $5mgl^{-1}$,8.0×10^8 CFU/mL and 7.0 respectively at a fixed benzene concentration of 200 mg/L and thereafter used in succeeding experiments of C-PBBR. Kureel et al 2016 reported a similar results in which benzene was treated with *Bacillus* species M_4 in a batch bio-reactor. ANOVA analysis found that $p < 0.05$ and the average value of concentration and removal was 89.14 mg/L and 77.14% respectively, standard error (3) and deviation was 17.32 for removal.

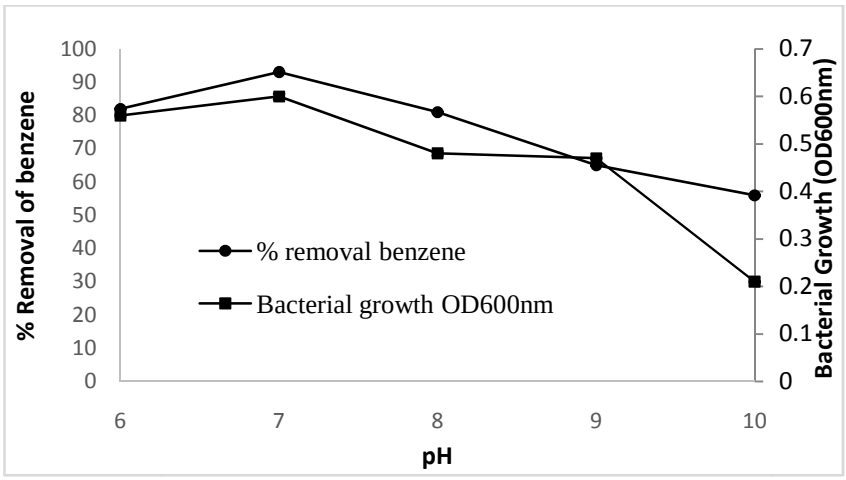

Fig 24(a) shows the removal efficiency with respect to inoculums size and bacterial growth

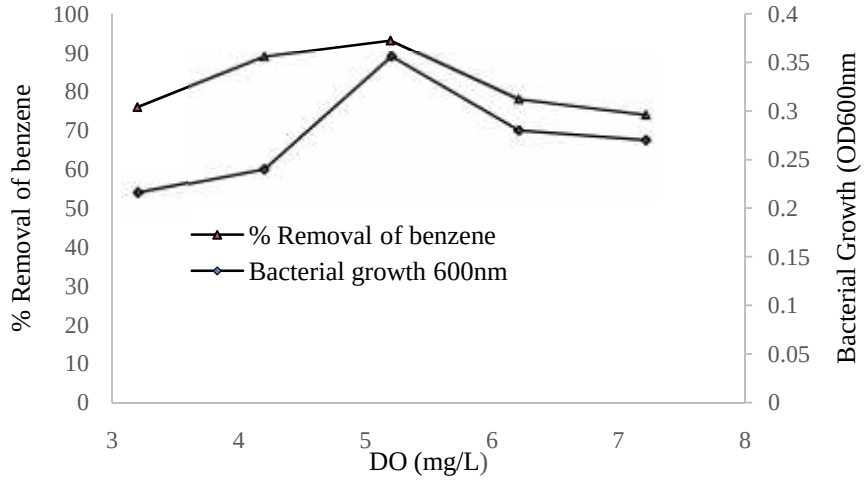

Fig.24(b) The removal efficiency with respect to DO and bacterial growth

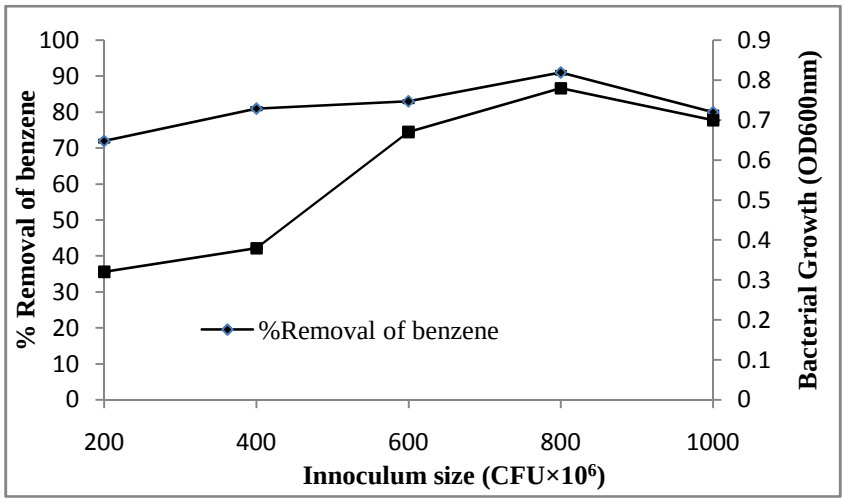

Fig.24 (c) The removal efficiency with respect to pH and bacterial growth.

3.8 Continuous packed bed bioreactor: performance evaluation

For adaptation by bacterial isolates and growth of bio-film on polyurethane foam requires approximately 20 days. SEM analysis was examined to confirm the growth of stable bio-film on the surface of PUF. The formation of bio-film reduces toxicity of pollutants and enhances the functional strength of the bio-reactor. Similar types of results were reported in other studies for bioremediation of various organic pollutants in bio-reactor (Tomei *et al*., 2004; Patil *et al*., 2006). In start-up period the bioreactor achieved supposed level of bio-film development through utilizing benzene and glucose as carbon source (Shawaqfeh, 2010).

At start-up, the C-PBBR was run with changing feed-flow rate (10 to50 mL/h) with 400 mg/L initial benzene concentration to explore the changes in inlet, outlet concentration and removal efficiency with respective to operating time (day) as depicted in (Fig.25) and **Table 7**. On 21st day the feed-flow rate was 10 mL/h (EC 28.8 mg/L/d and loading rate of 96 mg/L/d) and a removal efficiency of 3.44% was observed with inlet and outlet

concentration of 290 and 280 mg/L, respectively. With the increase in operating time, RE also increased and on 40th day maximum removal of 91.81 % was noticed. On the 40th day of operation the inlet benzene concentration was 391mg/L and outlet was 32 mg/L. After 40th day, the removal efficiency started decreasing and became steady (RE 79%) during 44th - 46th days of performance. This might be due to substrate inhibition and toxic environment by intermediates (Kureel et al 2016, Geed et al 2017, Shukla et al 2010). The flow rate of feed was increased to 20 mL/h (EC 156 mg/L/d and loading rate 192 mg/L/d) on the 47th day. As a result the % removal increased from 80.56% to 93.13% in the 47-54th day of operation and then started decreasing till 60th day and became steady with 77.83 % (RE) during 60th to 62th day. On 60th day the inlet-outlet concentration was 370 mg/L and 82 mg/L respectively. The flow rate of feed was raised to 30 and 40 mL/h on 63th and 75th day as a result of which maximum % removal of 89% and 84% was noted respectively and then achieved steady values on 72nd and 89th day of operation as depicted in (Fig.25 and **Table 7**). With flow rate of feed at 30 and 40 mL/h, the elimination capacity and loading rate were 234, 312 mg/L/d and 288, 384 mg/L/d, respectively. On comparison it can be seen that % removal was greater for flow rate of 20 mL/h than 30 and 40 mL/h however more elimination were observed at higher flow rates. The cause for this lies in residence time (RT) as RT of 20mL/h is greater than 30 and 40 mL/h. Previously researchers have recorded that the RT in the bio-reactor might not be so important for the substrate mineralization (Tsai et al 2013, Singh et al 2006, Shukla et al 2010). At 50 mL/h of flow rate the benzene RE was 66.92%, with inlet concentration of 387 mg/L and outlet concentration of 128 mg/L on 99th day and afterwards became steady upto 104th running day with corresponding EC and loading rate of 480 mg/L/d and 324 mg/L/d. The result

show that even at very high loading rate the bioreactor is performing relatively well as compared to previous work (Geed et al, 2017, Kureel et al., 2016; Singh et al., 2010).

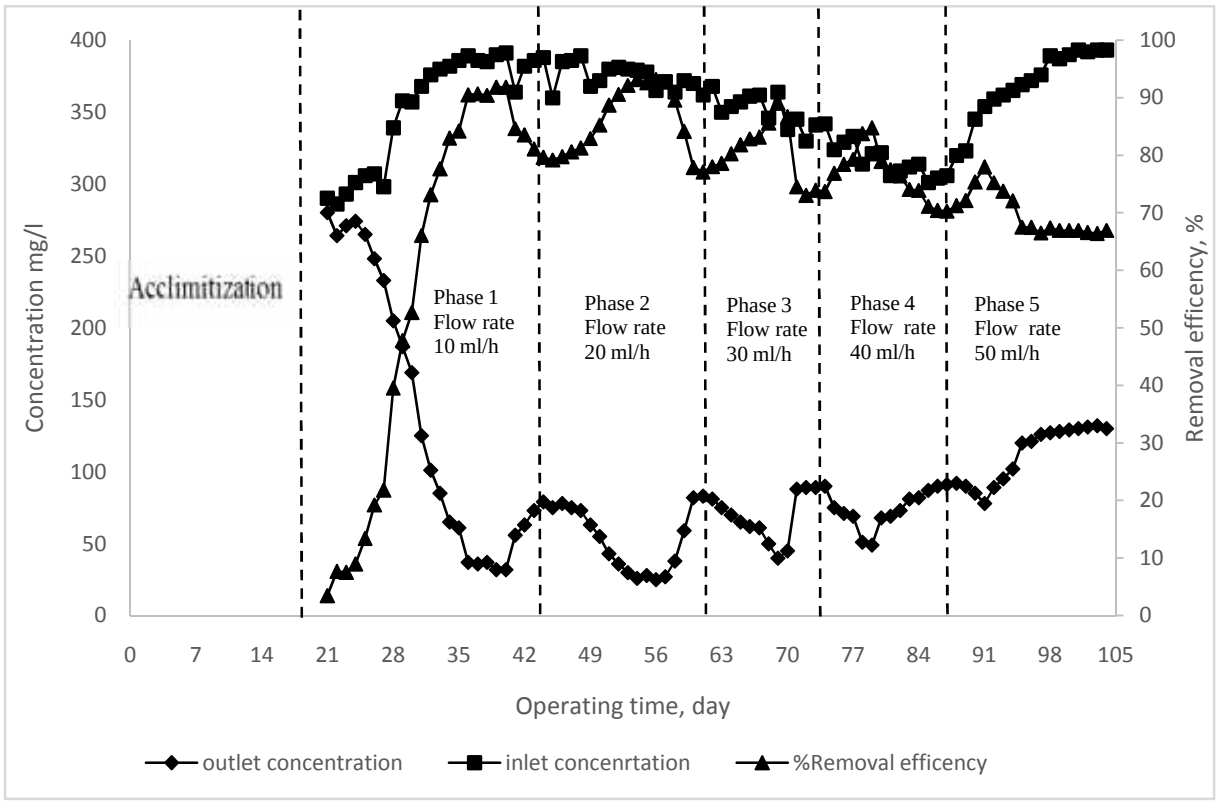

Fig 25: The performance of bioreactor at various feed flow rate (10-50 mL/h)

Table7: Effect of parameters on performance of continuous packed bed bioreactor using *Bacillus* sp. M4.

Flow rate (mL/h)	Operation days	% RE range	EC range (mg/L/day)	Loading rate (mg/L/day)
10	26	3.44-91.81	28.8-88.32	96
20	16	77.07-93.13	152.12-180	192
30	12	73.03-89.01	223.2-259.2	288
40	13	70.26-84.73	296.64-336.96	384
50	17	66.41-77.76	321.6-386.4	480

Fig 26 depicted the effect on inlet RE, EC and loading rate in CPPBR. The graph indicated that RE increased up to the loading rate 192 mg/L/d and corresponding EC 156 mg/L/d was notice. Above that the RE started decreasing and attained 77.96 mg/L/d while EC increased continuously up to 369.6 mg/L/d. This type of phenomenon was expressed by various researchers (Cooper et al., 2016; Kureel et al., 2016; Geed et al., 2017) in packed bio-reactor which might be caused because of change in rate-controlling mechanism. In the current work with inlet loading rate at 192 mg/L/d, the rate determining step changed from mass transfer to bio-reaction zone. Below critical benzene loading rate the diffusion to biomass was low which led to mass transfer limitations. At high loading rate, its mass-transfer rate from the bulk of liquid to bio-film increased and thereby sufficient benzene concentration would be available for the biomass. Under these conditions, removal of benzene depends on the capacity of bacteria to metabolize available benzene (Kureel et al., 2016) .The operation might be controlled by the degradation kinetics. The various reasons that might be responsible for the decrease in removal at high loading rates are bacterial plugging on the surface of packing media, bypassing due to excess growth of biomass on PUF, very less contact time between benzene, substrate and substrate inhibition (Halim et al., 2016; Geed et al., 2017).

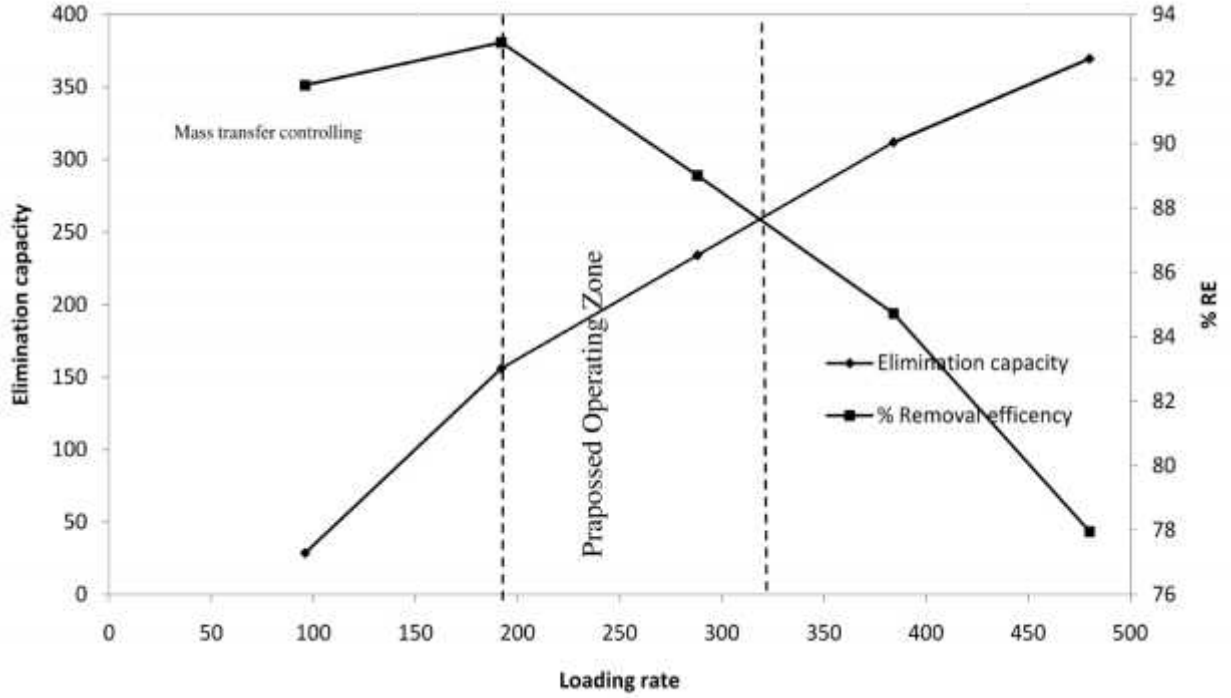

Fig 26 The variation of removal efficiency (% RE) and elimination capacity (mg/L/day) with respect to loading rate (mg/L/day)

3.9 Residual Analysis: GC, FT-IR and GC-MS

In order to know the inlet and outlet benzene concentration, GC analysis was carried out. The control benzene sample in absence of inoculums was separately run with corresponding peak at 3.2 min RT. Similar investigation was done for inlet-outlet concentration of benzene.

From the FTIR outcomes, peaks of 3345.1 to 3400.3 1/cmand 1643.3 (1/cm) confirmed hydroxyl (-OH) and carbonyl groups (=CO) presence. This clearly indicates of the successful bio-oxidation of benzene in aqueous phase. Along with above mentioned groups, certain peaks from 662.4 to 3994.1 (1/cm) which corresponded only with Benzene-1.2-diol was obtained. The stable metabolite formed as a result of the degradation of benzene may be associated with the additional group. However for the confirmation of results further

investigation was done which required usage of technique such as GC-MS. Benzene's band spectrum was 1815.0 (1/cm) for the control sample Fig 27a The outcomes were in accordant with those described by Robledo-Ortíz et al. (2011)(Fig27b). This functional group corresponded to the metabolite formed in degradation of benzene.

The outcomes were in accordace with those described by Singh and Fulekar, (2010) who also noticed similar functional groups by FTIR. The FTIR results indicate that the *Bacillus* species M_4 follow a particular metabolic pathway for benzene bio-remediation (Robledo-Ortiz et al., 2011; Padhi and Gokhale, 2017). In order to confirm the results, further investigation was done which required techniques like GC-MS. The biodegraded benzene samples extracted by *n*-hexane at the end of 104^{th} day were analysed by GC-MS. The GC-MS outcome showed that benzene-1,2-diol was an intermediate in aerobic oxidation by isolated *Bacillus* species M4 which was in accordance with FTIR findings. The GC-MS chromatographic result of as controlled benzene and metabolite formation during degradation process was shown in(Fig.28a) and (Fig.28b) **Table 8(a, b)** respectively.

The benzene-1, 2-diol was considered as a major intermediary of aerobic benzene degradation, in which mineralization of carbon took place resulting in electron ejection which support biomass growth (Yu et al., 2001; Jindrova et al., 2002; Singh and Fulekar 2010

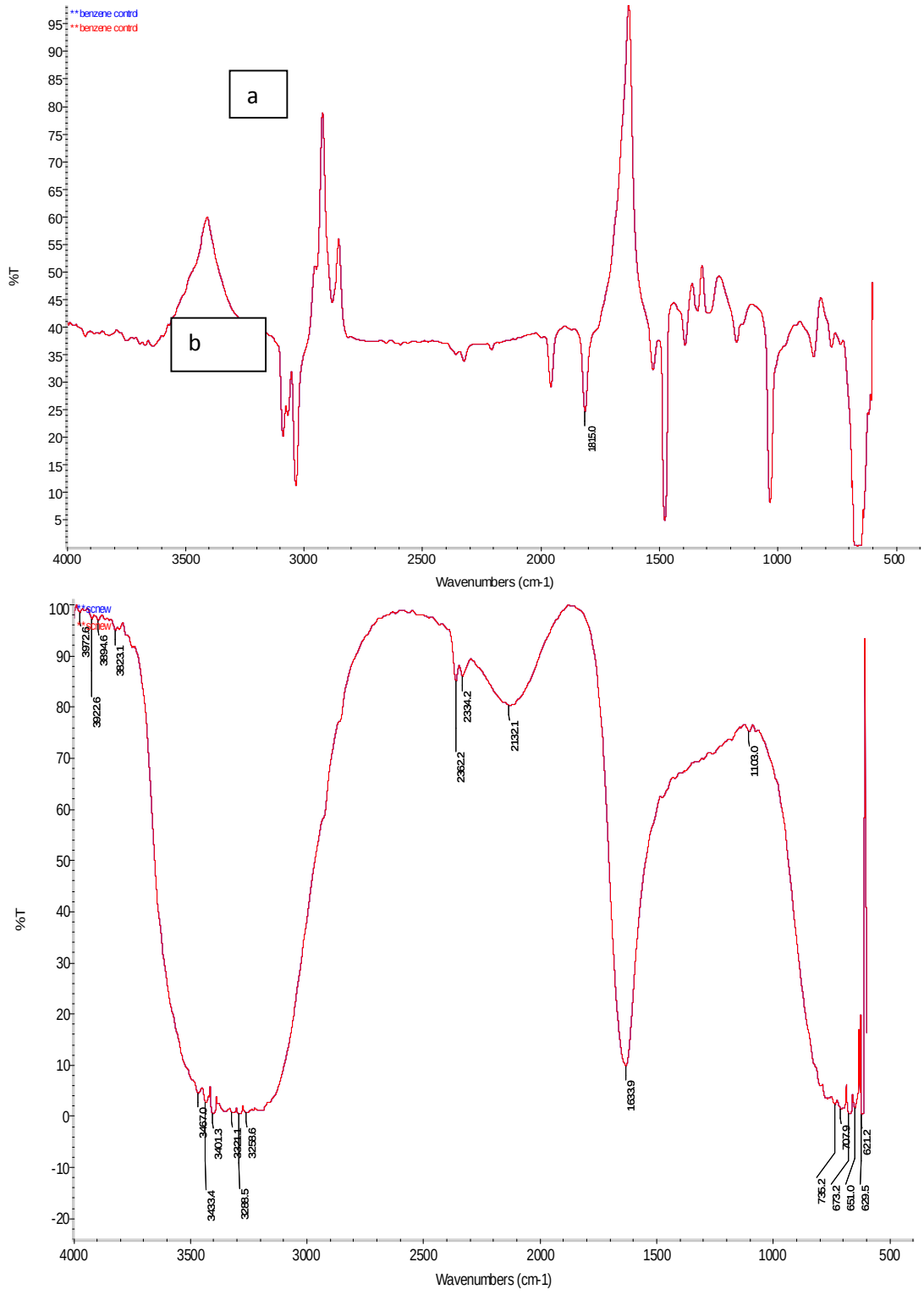

Fig 27: (a) control benzene (b) formation of metabolite (Benzene-1.2-diol) in biodegraded sample of benzene

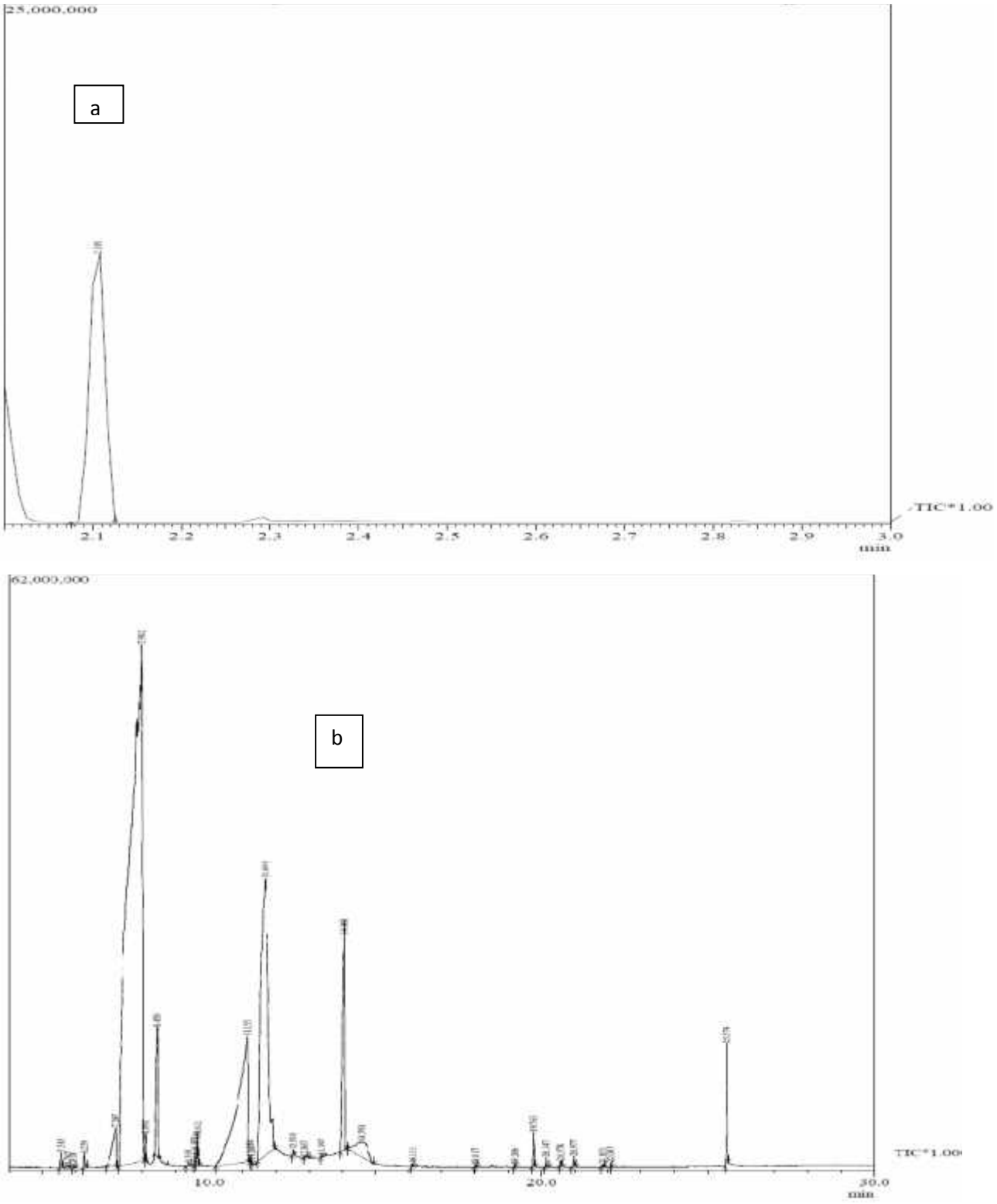

Fig 28: GC-MS result of (a) control of benzene (b) formation of one metabolite Benzene-1.2-diol in biodegraded sample of benzene

Table 8a: Shows GC-MS Result of Control benzene

Peak#	R.Time	Area	Area%	Name
1	2.105	16231435	100.00	Benzene
		16231435	100.00	

Table 8b: shows GC_MS Result of Benzene Metabolites

Peak#	R.Time	Area	Area%	Name
1	5.543	2756580	0.11	Acetic acid, 3-methoxy-2-butyl ester
2	5.745	633789	0.03	4-Cyclopentene-1,3-dione
3	5.918	439406	0.02	BUTANOIC ACID, 3-OXO-, METHYL ESTER
4	6.259	2962374	0.12	METHYL 2,2-DIMETHOXYPROPANOATE
5	7.207	32153453	1.33	3-METHYL-2,5-FURANDIONE
6	7.982	1445893889	59.89	Carbamic acid, phenyl ester
7	8.091	2461015	0.10	2-Furanone, 2,5-dihydro-3,5-dimethyl
8	8.450	50288432	2.08	Butanedioic acid, dimethyl ester
9	9.395	827536	0.03	cis-2-Methyl-2-butenedioic acid, dimethyl ester
10	9.573	2487286	0.10	2,5-FURANDIONE, 3-ETHYL-4-METHYL-
11	9.638	1319045	0.05	Carbonic acid, 2-methoxyethyl phenyl ester
12	9.672	2467124	0.10	Carbonic acid, 2-methoxyethyl phenyl ester
13	11.155	270352733	11.20	Butanedioic acid, monomethyl ester
14	11.238	552598	0.02	PENTANEDIOIC ACID, MONOMETHYL ESTER
15	11.297	330027	0.01	Pentanedioic acid, monomethyl ester
16	11.694	420721467	17.43	BENZENE-1,2-DIOL
17	12.530	1665241	0.07	5-Hydroxy-4,5-dimethyl-2,5-dihydrofuran-2-one
18	12.867	1019655	0.04	2-ISOPROPYL-5-METHYL-PHENOL
19	13.397	526994	0.02	Cyclooctanol, acetate
20	14.068	96681964	4.00	2,3-DIHYDRO-1,4-BENZODIOXIN-2-YLMETHANOL #
21	14.591	42526985	1.76	Butanedioic acid
22	16.131	513126	0.02	Phenol, 2-phenoxy-
23	18.017	296116	0.01	TETRADECANOIC ACID, METHYL ESTER
24	19.206	410468	0.02	1-TERT-BUTYL-2-METHOXY-4-METHYL-3,5-DINITRO
25	19.763	5865547	0.24	4-Hydroxy-6-methyl-3,4-dihydro-2(1H)-pteridinone
26	20.147	1539478	0.06	HEXADECANOIC ACID, METHYL ESTER
27	20.578	1190179	0.05	HEXADECANOIC ACID
28	20.977	2252239	0.09	N-[2-(2-THIENYL)ETHYL]-1-ADAMANTANECARBOX
29	21.851	440700	0.02	9-OCTADECENOIC ACID, METHYL ESTER, (E)-
30	22.085	707456	0.03	OCTADECANOIC ACID, METHYL ESTER
31	25.574	22014111	0.91	1,2-BENZENEDICARBOXYLIC ACID
		2414297013	100.00	

3.10 Proposed metabolic pathway for benzene biodegradation

The capability of a micro-organism to degrade compound lies in its ability to produce enzymes which as biocatalyst and make the bio-reactions possible (Chaudhry, 1994). The break down efficiency was influenced by the accessibility of compound to enzyme. An enzyme's Performance is defined on its catalyzing power and production capacity by the micro-organisms (Chaudhry, 1994). The degradation of benzene and other similar aromatic compounds into non-toxic intermediates of tricarboxylic acid (TCA) cycle by *Bacillus species.*, *Pseudomonas species* etc. have been reported by many researchers (Singh and Fulekar, 2010;Banerjee and Ghoshal, 2010). Present work provides a proposed pathway for benzene degradation in presence of oxygen via three step 1,2 and 3 is shown in Fig.29.Wengen Zhou et al 2016 reported degradation of benzene to phenol by toluene-4 monooxygenase enzyme. In present study formation of benzene-1, 2-cis, cis –dihydrodiol metabolites by dioxygenase enzyme was noticed which was earlier discussed by (Fritsche et al 2000). In benzene degradation, benzoate was found as an intermediate product. In the production of benzene-1, 2-diol from benzene 1,2 cis-cis-dihydrodioldehydrogenase enzyme might have played a key role (Zeyaullah et al 2009 Smith, 1990, Fritsche et al 2008). During degradation, phenol 2-monooxygenase attacked the preexisting -OH group at ortho position to generatebenzene-1, 2-diol, followed by catalyzation with catechol 1, 2-dioxygenase to generate acetyl-CoA and succinic acid (Pandeeti and Siddavattam, 2011, Wengen Zhou et al 2006).By step 5 benzene-1, 2-diolwas degraded to acetaldehyde and pyruvate by 2,3-dioxygenase (Mason and Cammack, 1992; Tuan et al., 2011). In the mid-pathway, formation of benzene-1, 2-diolto 2-hydroxy-muconic semialdehyde (HMS) was catalysed by C23O , which entered into the hydrolytic or 4-oxalocrotonate branch (Arai et al., 2000). In 4-oxalocrotonate branch of Common astestosteroni TA441, HMS was

transformed to 2-oxopent-4-dienoate subsequently by3 enzymes, i.e. 4-oxalocrotonatedecarboxylase (4OD), 4-oxalocrotonate isomerase (4OI), and 2-hydroxy-muconic semialdehyde dehydrogenase (HMSD). The hydroxylation of metabolin 2-oxopent-4-dienoate was done by 2-oxopent-4-dienoate hydratase (OEH) to yield 4-hydroxy-2-oxovalerate, which was further transformed to acetaldehyde and pyruvate by 4-hydroxy-2-oxovalerate aldolase (HOVA). Additionally, pyruvate can indulge in the tricarboxylic acid cycle and acetaldehyde dehy-drogenase (AcDH) converts acetaldehyde to acetyl-CoA eventually. Catechol which wass one of the metabolites can be transformed to cis-cismuconate throug enzyme catechol 1, 2-dioxygenase (C12O) which further enters the orthopathway. 3-oxoadipate enol-lactonasecatalyse, Muconate cyclo-isomerase and mucono-lactone isomerase converts cis-cismuconate to 3-oxoadipate that further gets transformed to acetyl-CoA and succinic acid. (Arai et al., 2000; Murray et al., 1972). Interestingly, ortho or meta-pathway can also be used to degrade aromatic compounds like carbazole, toluene and benzene (Jindrová et al., 2002; Shi et al., 2015).

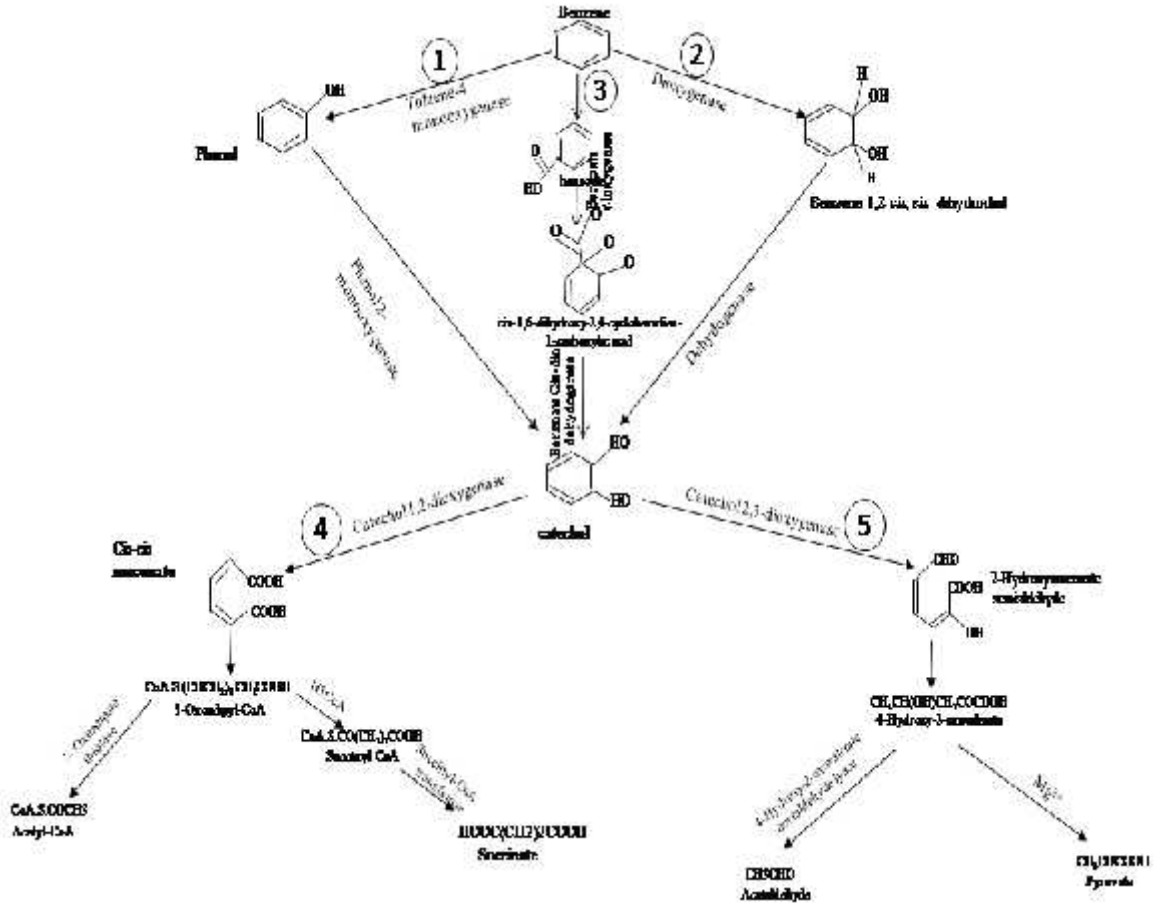

Fig 29: Study of Degradation pathway of benzene

3.11 2-D gel electrophoresis and MALDI-TOF MS/MS analysis

A total 275 protein spots were identified from control as well as treated gel by using PD Quest^{TM} basic version of 8.0.1 of which 127 and 90 were commonly up and down accumulated, 45 accumulated only in treated and 13 only found in control (Fig.30a). Most of the protein spots identified are in molecular weight range of 100-10 kDa and in*pI* range of 3-10.The results of 2DE clearly demonstrates that there is registered change in protein profile of *Bacillus* sp M4. on treatment with benzene, however 20 spots marked only on gel and 6 gel spot used for MALDI-TOF-MS/MS analysis (4 from control and 3 from treated).

It was investigated that protein spot should be identifiable as differentially expressed proteins in the protein profile of *Bacillus* sp. Hence, the treated and control cell extracts were analyzed by 2-D electrophoresis. Several protein bands were found as shown (Fig.30b and Fig.30c).

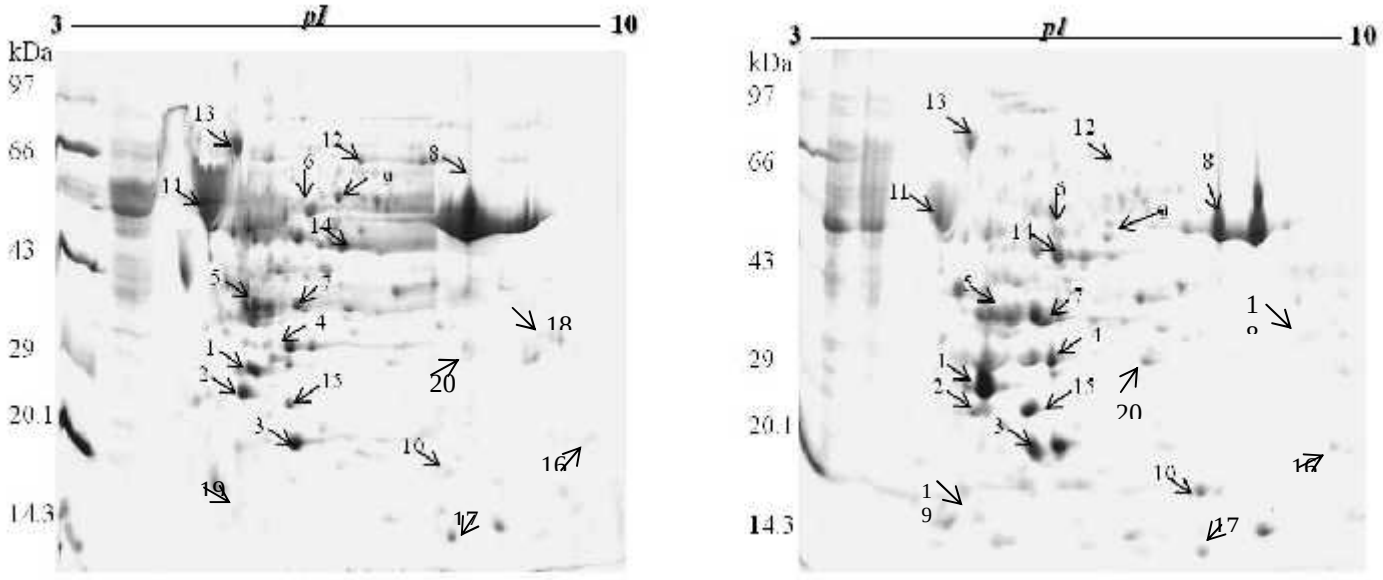

Fig 30:2DE gel image of (a) Control benzene (b) treated by *Bacillus* sp M4

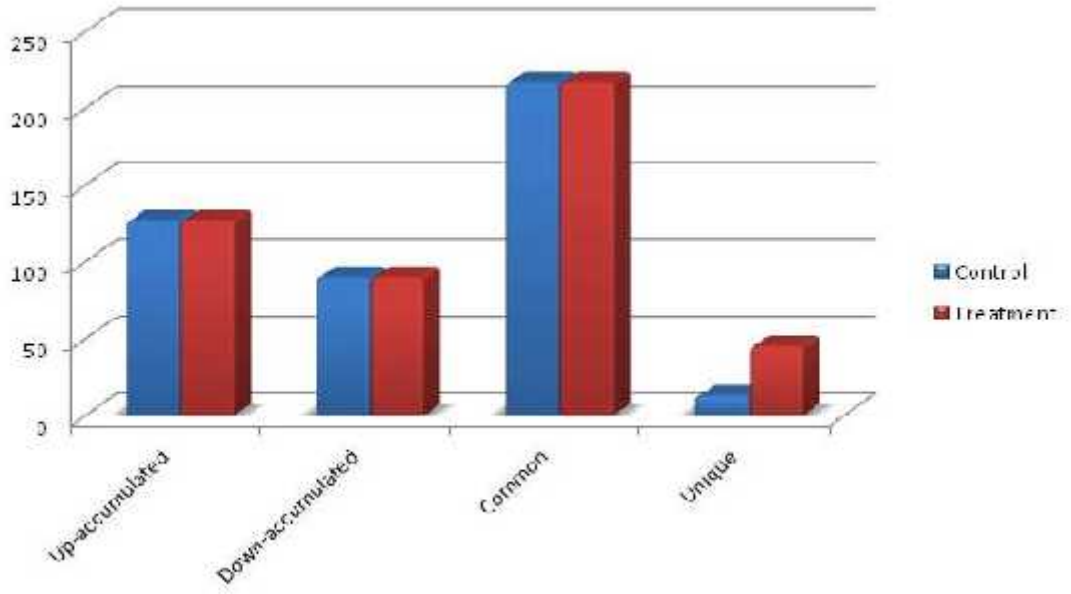

Fig 30c: Bar-diagram of proteins

3.12 In silico analysis and characterization of identified protein

3.12.1 *Functional domain analysis, Phylogenetic analysis,*

Total 7 proteins were identified using MALDI results. Out of 7 identified proteins, 2 hypothetical proteins were observed. To study their functional role of hypothetical proteins and identified proteins, *in silico* analysis were performed using bio informatics tools and server for characterization. The functional domain details were obtained from PFAM server and reported in **Table 9**. The 5 known proteins (2Fe-2S ferredoxin-type iron-sulfur binding region signature, ABC transporter, methionine ABC transporter (ATP-binding protein), Peptidase S24-like, Polyketide synthase dehydratase). 2Fe-2S ferredoxin-type iron-sulfur binding region signature protein involved in iron-deficient growth of the cyanobacterium Synechococcus sp. and high-affinity iron uptake in yeast (Reddy et al., 1988). ABC transporter protein controlling and methionine ABC transporter (ATP-binding protein)

Streptomyces fradiae tylosin resistance and ATP-binding transport and Crystal structure of the ATP-binding subunit of an ABC transporter (Hung et al., 1998). Peptidase S24-like plays role in protein domain annotations on fly (Marchler-Bauer and Bryant, 2004) and Polyketide synthase dehydratase protein involved in tolerance and Specificity of Polyketide Synthases (Khosla et al., 1999).

Table 9 domain functional analysis

S.N.	Protein ID	Protein Name	Interproscan; Prosite; CDD; SMART; Pfam	References
1.	NP_391706.1 Bacillus subtilis	2Fe-2S ferredoxin-type iron-sulfur binding region signature	(PF09375); EfeO; with user query added Superfamily	(Reddy et al 1988; Dancis, 1998;
2.	NP_389107.1 Bacillus subtilis	ABC transporter	ABC_tran;(PF00005); ATP-binding domain of ABC transporters	(Rosteck et al 1991; Blight and Holland, 1990;
3.	ZP_06874203.1 Bacillus subtilis	methionine ABC transporter (ATP-binding protein)	ABC_tran ; (PF00005); ABC transporter, NIL;(PF09383); C-terminus of ABC transporter proteins involved in D-methionine transport	Hollenstein et al 2007; Rosteck et al 1901;
4.	NP_389324.1 Bacillus subtilis	Peptidase S24-like	Peptidase_S24; (PF00717); Peptidase S24-like	Marchler-Bauer A et al. (2017),
5.	AHB03697.1	Polyketide synthase dehydratase	PS-DH; (PF14765); Polyketide synthase dehydratase PP-binding; (PF00550); Phosphopantetheine attachment site ketoacyl-synt; (PF00109); Beta-ketoacyl synthase, N-terminal domain	Khosla et al (1999); Jenke-Kodama et al 2005);
6.	ZP_03590478.1	hypothetical protein Bsubs1_04423	MS_channel; (PF00924); Mechanosensitive ion channel	Kloda and Martinac, 2001 Kloda et al 2001; Martinac , 2001
7.	BAI84687.1 Bacillus subtilis	hypothetical protein BSNT_07572;Predicted Zn-dependent protease YjaZ, DUF2268 family	DUF2268; (PF10026); Predicted Zn-dependent protease	Pryor et al, (2013); Quigley et al, (2013);

Similarly for 2 identify hypothetical protein were characterized by (Interproscan, Prosite, CDD and Pfam) server. First hypothetical protein (ZP_03590478.1)was showed fictional role MS channel (PF00924), structural and functional differences between two homologous mechano sensitive channels of Methanococcus jannaschii (Kloda et al., 2001). And second hypothetical protein (BAI84687.1) plays important role in structure of the integral membrane protein CAAX protease (Hung et al., 1998)

The tree construction was performed using MEGA 6 software. The phylogenetic classification of identified proteins was performed with similar or closely species related to bacillus cereus shown inFig.31.

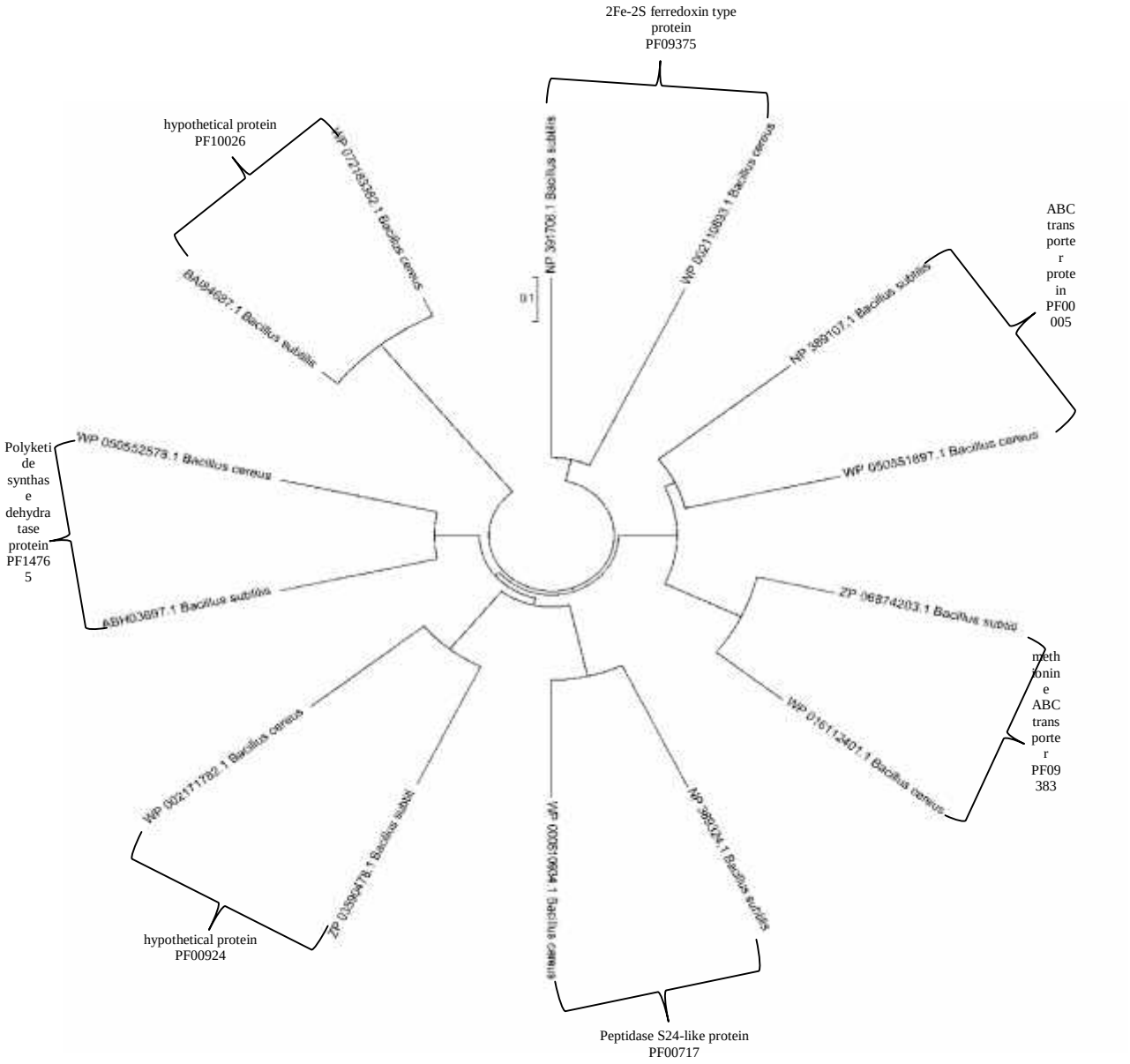

Fig 31: Phylogenetic tree identified protein**s**

The sequential classification revealed proper clustering along with bacillus cereus. Structures were constructed using Discovery Studio3.0 and Swiss Model shown in **Fig 32a** and **Fig 32b.**

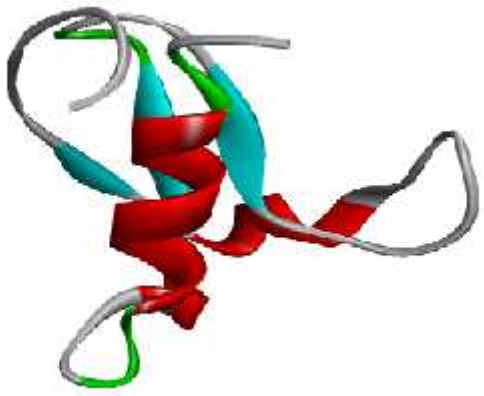

Fig. (32a): SWISS MODEL (BAI84687.1)

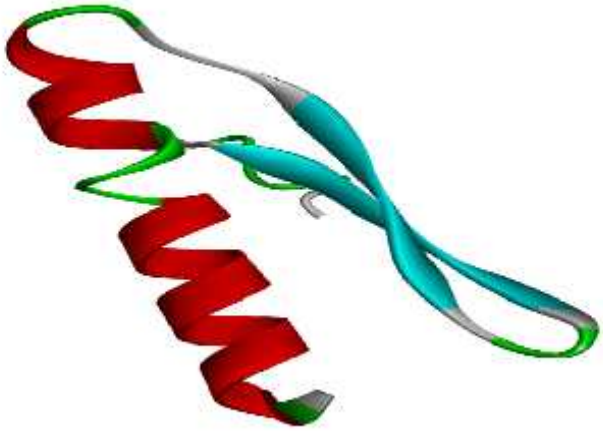

Fig. (32b): Discovery Model (BAI84687.1)

The best constructed structure was taken for verification. The detail of RAMPAGE statistics of predicted model obtained from Discovery Studio 3.0 and Swiss Model server were reported in **Table 10 (a)** and **Table 10 (b)**

Table .10a Models obtained by Discovery Studio 3.0 using RAMPAGE

Accession No.	Protein Name	Number of residues in favoured region (~98.0% expected)	Number of residues in allowed region (~2.0% expected)	Number of residues in outlier region
ABH03697.1	5. PksC	93.3%	4.5%	2.2%
BAI84687.1	7. Hypothetical protein BSNT	96.8%	3.2%	0.0%
NP_389107.1	2. ABC transporter ATP-binding protein	93.8%	3.5%	2.7%
NP_389324.1	4. signal peptidase I T	89.4%	4.2%	6.3%
NP_391706.1	1. IRON uptake system component EfeM	98.1%	1.9%	0.0%
ZP_03590478.1	6. hypothetical protein Bsubs1	89.1%	9.5%	1.4%
ZP_06874203.1	3. methionine ABC transporter	94.1%	5.3%	0.6%

Table.10b. Models obtained by Swiss Model using RAMPAGE

Accession No.	ProteinName	Number of residues in favoured region (~98.0% expected)	Number of residues in allowed region (~2.0% expected)	Number of residues in outlier region
ABH03697.1	5. PksC	95.2%	3.8%	1.0%
BAI84687.1	7. Hypothetical protein BSNT	88.9%	11.1%	0.0%
NP_389107.1	2. ABC transporter ATP-binding protein	88.5%	5.3%	6.2%
NP_389324.1	4. signal peptidase I T	95.1%	4.9%	0.0%
NP_391706.1	1. IRON uptake system component EfeM	97.7%	2.3%	0.0%
ZP_03590478.1	6. hypothetical protein Bsubs1	91.0%	5.2%	3.8%
ZP_06874203.1	3. methionine ABC transporter	91.2%	6.5%	2.4%

3.13 Active side analysis and Docking

Best predicted model have selected spot no 5 treated with benzene which having good quality structure for docking calculation as shown in Fig.33aandFig.33b. Prior to docking calculation active binding sites were identified using META pocket server. The details of active binding sides were given in **Table .11(a).**

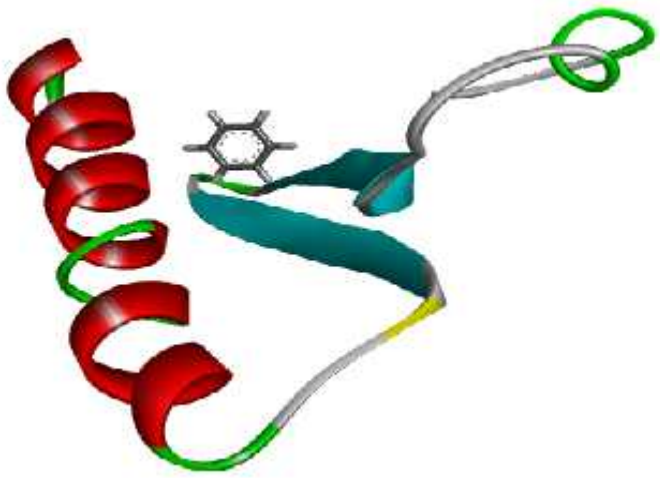

Fig. 33a: Protein Docking with Benzene

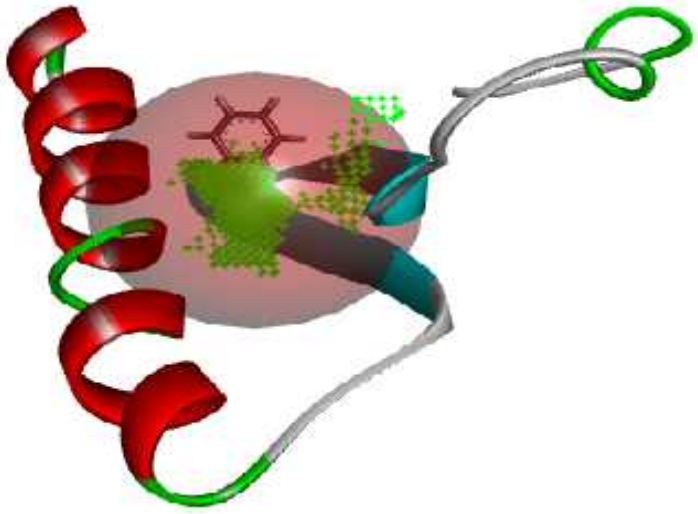

Fig. 33b: Active site protein docking with Benzene

Docking calculation study revealed that residuesARG98, ARG 99, ILE 100 ,GLY 109, LEU110, MET133, THR134 and TYR137, as shown in Fig 31c.These residues which were involved in interaction of measure active binding sites MEGA pocket **Table.11(b)**with binding energy 4.1930 kcal/mole and dissociation constant 844287296 PM.

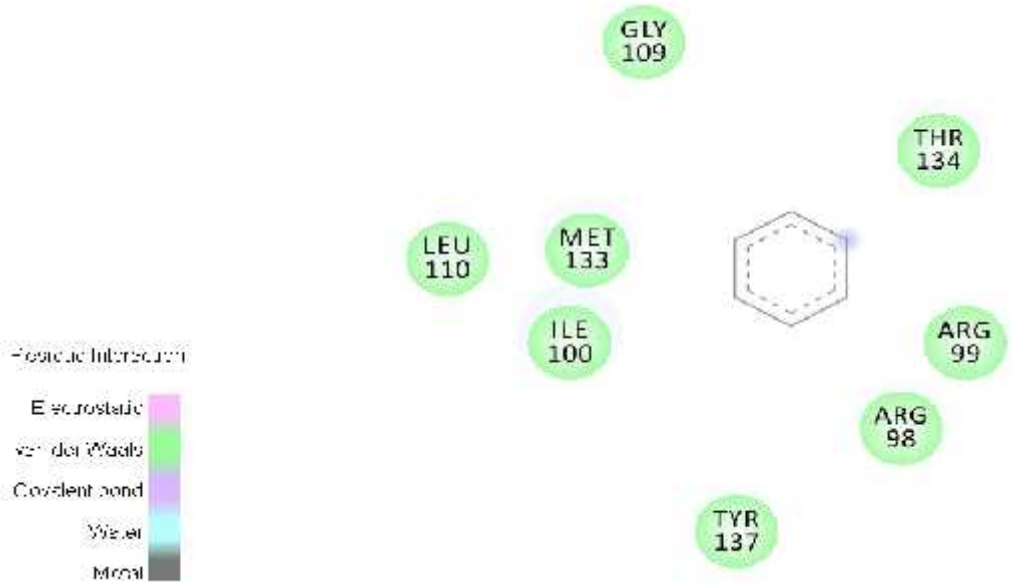

Figure 33c: Major active site and residual interaction

Table: 11a Major active side and Docking

ABS	AB RESIDUES
SITE 1	GLN^{113}, MET^{116}, SER^{122}, ASP^{125}, PHE^{126} LEU^{110}, ALA^{111}, GLY^{109}, SER^{121}, SER^{130} GLU^{95}, PHE^{112}, ALA^{131}, THR^{134}, SER^{108} ARG^{99}, ARG^{98}, VAL^{129}, ASN^{97}, MET^{133} ILE^{100}, LEU^{132}, ARG^{101}, LYS^{107}, TYR^{137} HIS^{138}, CYS^{141},
SITE2	LYS^{80}, TRP^{81}, GLN^{82}, VAL^{86}, PRO^{92} VAL^{93}, ASP^{85}, VAL^{89}, ILE^{88}
SITE3	PHE^{119}, LEU^{120}, ASP^{123}

Table: 11b Docking calculation, binding energy, dissociation constant and residue

Clu No.	Binding energy[kcal/mol	Dissociation constant [pM]	Contacting receptor residues
001	000004.1930	00000844287296.0000	ARG98, ARG99, ILE100, GLY109, LEU110, MET133, THR134, TYR137,
002	000003.4150	00003138859008.0000	GLU95, ALA111, PHE112, GLN113, MET116, SER122, ASP125, PHE126, SER130,
003	000003.4070	00003181529088.0000	LYS80, TRP81, GLN82, ASP85, VAL86, VAL89, LEU91, PRO92, VAL93,
004	000003.0680	00005638014464.0000	ARG99, ILE100, ARG101, SER108, GLY109, LEU110,
005	000002.8680	00007901837824.0000	ASN97, ARG98, ARG99, LEU110, ALA111, PHE112,
006	000002.8130	00008670490624.0000	ARG98, SER128, VAL129, LEU132, MET133, GLU136,TYR137,
007	000002.7340	00009907211264.0000	ASP94, GLU95, GLN113, SER121, LEU124, ASP125, VAL129,
008	000002.6910	00010652973056.0000	GLU136, TYR137, VAL140,
009	000002.5870	00012697079808.0000	LEU91, ASP94, GLN113, LYS115, MET116, PHE117,

3.14 Structure predictions of other identified proteins

Design and structural prediction of the others proteins with the help of Discovery software 3.0 and Swiss model which were not used in docking with benzene shown in **Fig 34(a-g).**

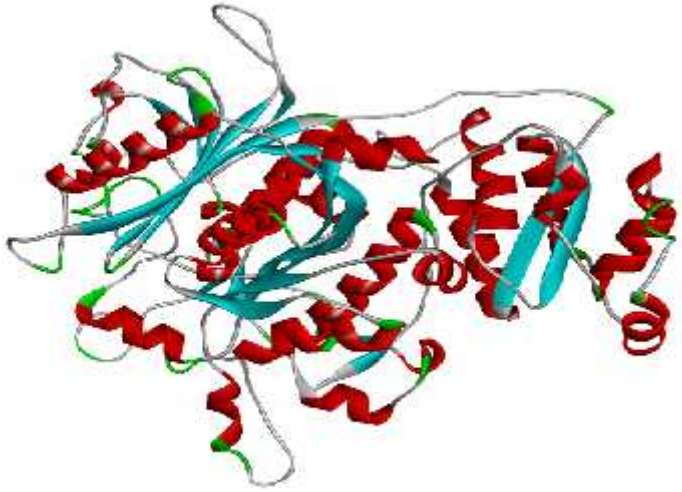

Fig. 34(a): The structure of design by discovery model ABH03697.1

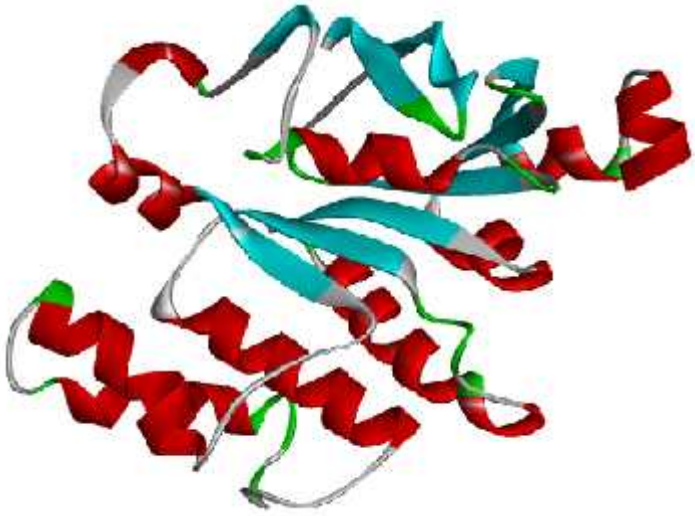

Fig. 34(b): The structure of design by discovery model NP_389107.1

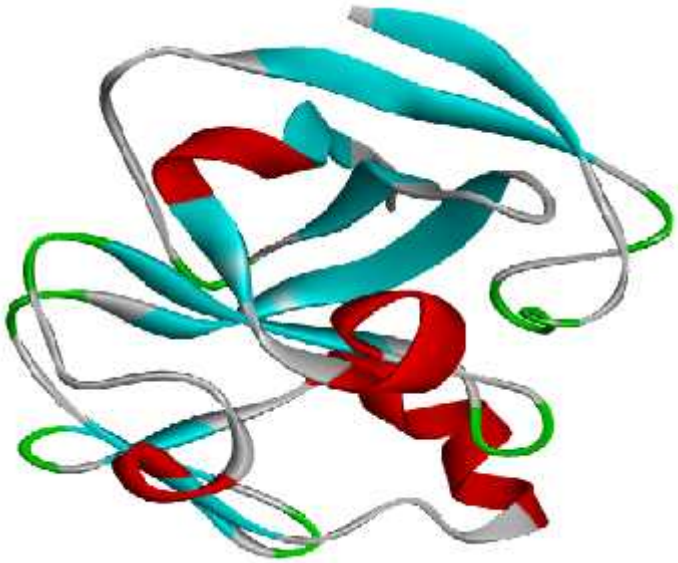

Fig.34(c): The structure of design by discovery model NP_389324.1

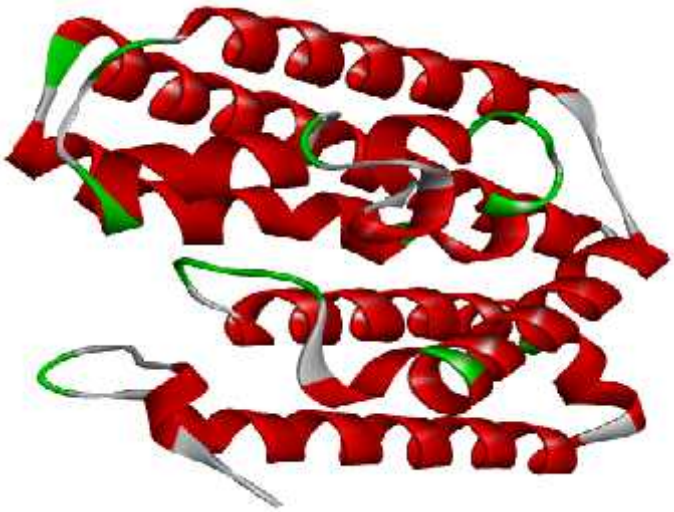

Fig. 34(d): The structure of design by discovery model NP_391706.1

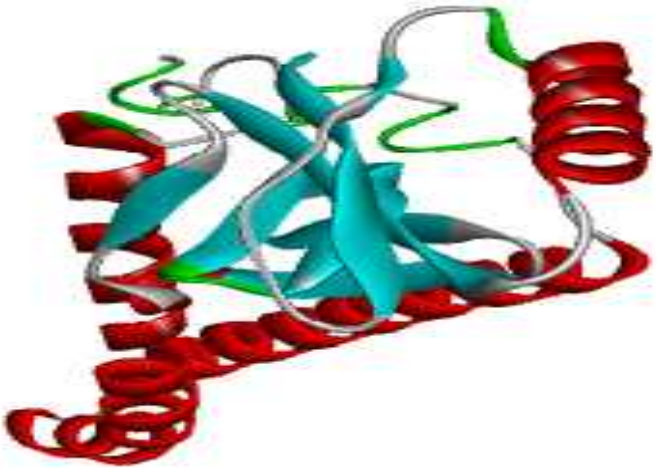

Fig.34 (e):The structure of design by discovery model ZP_03590478.1

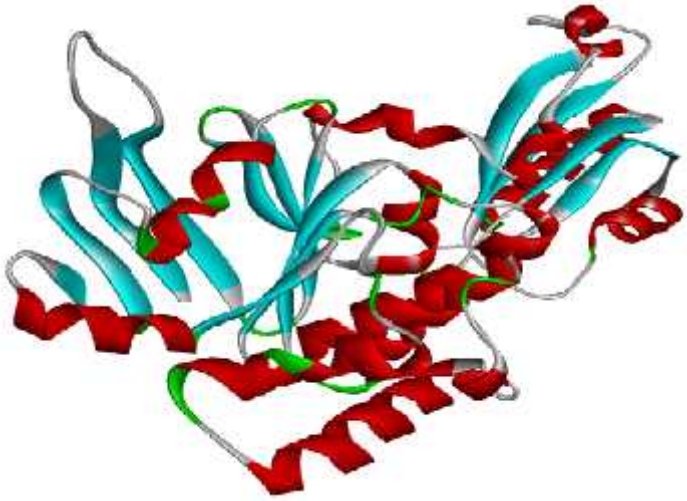

Fig. 34 (f): The structure of design by discovery model ZP_06874203.1

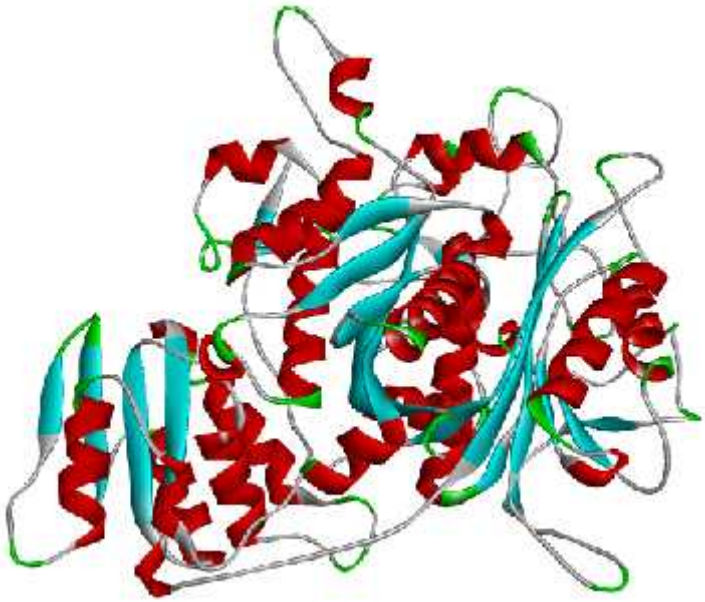

Fig. 34(g): The structure of design by discovery model ZP_06874203.1

Chapter 4
Conclusion